~~CONFIDENTIAL~~ UNCLASSIFIED

Copy 5 c.1
RM L51D24

NACA RM L51D24

JUL 3 1951

NACA

RESEARCH MEMORANDUM

PRESSURE-DISTRIBUTION MEASUREMENTS OVER A 45° SWEPTBACK WING AT TRANSONIC SPEEDS BY THE NACA WING-FLOW METHOD

By Edward C. B. Danforth and Thomas C. O'Bryan

Langley Aeronautical Laboratory
Langley Field, Va.

CLASSIFICATION CANCELLED

Authority NACA R7 2625 Date 8/31/54

By MXH 9/15/54 See

FOR REFERENCE

NOT TO BE TAKEN FROM THIS ROOM

CLASSIFIED DOCUMENT

This document contains classified information affecting the National Defense of the United States within the meaning of the Espionage Act, USC 50:31 and 32. Its transmission or the revelation of its contents in any manner to an unauthorized person is prohibited by law.
Information so classified may be imparted only to persons in the military and naval services of the United States, appropriate civilian officers and employees of the Federal Government who have a legitimate interest therein, and to United States citizens of known loyalty and discretion who of necessity must be informed thereof.

NATIONAL ADVISORY COMMITTEE FOR AERONAUTICS

WASHINGTON
June 25, 1951

NACA LIBRARY
LANGLEY AERONAUTICAL LABORATORY
Langley Field, Va.

~~CONFIDENTIAL~~
UNCLASSIFIED

NASA Technical Library
3 1176 01436 8618

UNCLASSIFIED

NATIONAL ADVISORY COMMITTEE FOR AERONAUTICS

RESEARCH MEMORANDUM

PRESSURE-DISTRIBUTION MEASUREMENTS OVER A 45° SWEPTBACK WING AT TRANSONIC SPEEDS BY THE NACA WING-FLOW METHOD

By Edward C. B. Danforth and Thomas C. O'Bryan

SUMMARY

Measurements of pressure were made over the chord of a swept-wing model at four stations along the span (2, 6, 50, and 82 percent semispan) by the NACA wing-flow method. The model tested was an untapered 45° sweptback wing of aspect ratio 3.5 with 2-inch-chord NACA 65-210 airfoil sections normal to the leading edge. The tests were conducted at Mach numbers from about 0.7 to 1.1 at angles of attack from -1° to 4°. The Reynolds number of the tests was nominally 0.6×10^6 based on the wing chord in the stream direction. The results are presented to show the chordwise pressure distributions and the spanwise distributions of section lift, drag, and pitching moment.

Little change in the spanwise lift distribution was found to occur between Mach numbers of 0.7 and 1.1. The spanwise center of pressure was between 45 and 50 percent semispan. The section pressure-drag coefficient was found to be a maximum at the wing root and to decrease along the span at all Mach numbers. At a Mach number of 0.90 the experimental and theoretical section pressure-drag coefficients showed similar variations along the span and were roughly of the same magnitude. At a Mach number of 1.05 agreement between the experimental and the theoretical section pressure-drag coefficients was obtained only near the wing root; at the more outboard stations the experimental drag coefficients were higher than the theoretical. Comparison of the data from this investigation with previously published wing-flow force-test measurements showed good agreement for the slopes of the wing lift and pitching-moment curves and the zero-lift wing drag coefficient at all test Mach numbers.

[redacted]

UNCLASSIFIED

INTRODUCTION

The study of the aerodynamic characteristics of sweptback wings in the transonic speed range has already received considerable attention. The studies to date, however, have been concerned primarily with the over-all characteristics obtained from force tests. Very little detailed information is yet available on the pressure distribution over swept wings or the spanwise lift and drag distributions through the speed of sound. Pressure distributions measured on swept wings at high subsonic speeds are reported, for example, in reference 1. References 2 and 3 report the pressure distribution over sweptback wings at supersonic speed.

In order to provide more detailed information on the flow about swept wings at transonic speeds, a program of pressure measurements has been conducted by the NACA wing-flow method. The model used in the investigation was an untapered 45° sweptback wing of 3.5 aspect ratio, with NACA 65-210 airfoil sections normal to the leading edge. Pressures have been measured at four spanwise stations at Mach numbers between 0.7 and 1.1 at a Reynolds number of about 0.6×10^{6} based on the chord in the stream direction. The pressure data are presented in terms of the section and over-all wing characteristics and have been compared with force-test and theoretical results where possible.

SYMBOLS

b	wing span
c	wing chord in stream direction
C_D	wing pressure-drag coefficient (D/qS)
c_d	section pressure-drag coefficient (d/qc)
C_{D_T}	total drag coefficient (pressure drag plus skin friction)
C_L	wing lift coefficient (L/qS)
c_l	section lift coefficient (l/qc)
C_m	wing pitching-moment coefficient about an axis through the center of area of semispan plan form (M/qcS)

c_m	section pitching-moment coefficient about an axis through the center of area of semispan plan form (m/qc^2)
D	wing pressure drag
d	section pressure drag
L	wing lift
l	section lift
M	Mach number; wing pitching moment about an axis through the center of area of semispan plan form
M_{av}	average stream Mach number over region occupied by model
M_l	local stream Mach number at position of orifices
M_R	Mach number at the wing root
m	section pitching moment about an axis through the center of area of semispan plan form
P	pressure coefficient $\left(\frac{p - p_o}{q}\right)$
p	local static pressure
p_o	free-stream static pressure (at model position)
q	free-stream dynamic pressure (at model position)
R	Reynolds number $\left(\frac{\rho V c}{\mu}\right)$
S	wing plan area
V	free-stream speed (at model position)
x	longitudinal distance along wing chord
y	lateral distance along semispan
α	angle of attack
α_o	angle of attack for zero lift

Λ sweep angle, degrees

ρ mass density of air

μ coefficient of viscosity of air

APPARATUS AND PROCEDURE

The airfoil (fig. 1) was mounted to extend into the high-speed air stream over a specially faired ammunition compartment cover on the wing of an F-51 airplane, as shown in figure 2. The curvature of this cover plate was selected to give small horizontal velocity gradients at the model position up to test Mach numbers of about 1.05. Typical distributions of Mach number on the surface of the cover plate in the region of the model and typical test Reynolds numbers are given in figure 3. The Mach number gradient normal to the airplane wing surface has been found to be about -0.007 per inch.

A sketch of the 45° sweptback semispan wing model mounted on the airplane wing is given in figure 4. The span of the model was 5 inches, measured from the airplane wing surface, and the chord in the stream direction was 2.83 inches. The corresponding aspect ratio was 3.5. The airfoil sections were of NACA 65-210 profile in planes perpendicular to the leading edge. The wing tip was cut off parallel to the stream direction and rounded slightly.

A circular end plate (figs. 2 and 4) with a diameter 1/2 inch greater than the streamwise chord of the model was provided near the wing root to minimize the effect of the airplane wing boundary layer on the flow over the model. The slot cut in the airplane wing surface to accommodate the model was sealed to prevent leakage.

The pressure distributions reported herein were obtained in planes parallel to the stream direction at distances of 0.35, 2.50, and 4.10 inches above the airplane wing surface (fig. 4). At each orifice plane, 16 orifices were provided on the upper surface and 15 on the lower surface, spaced from 3 to 90 percent chord as indicated in figure 4.

The description of the position of the orifice planes in terms of the model semispan is complicated by the fact that two series of measurements were made; one with the upper surface of the end plate 0.06 inch above the airplane wing and the other with the end plate 0.25 inch above. The positions of the two outboard orifice planes have been measured from the airplane wing surface while the position of the inboard orifice plane has been measured from the surface of the end plate. All

distances were expressed as fractions of the 5-inch semispan. On this basis, then, pressure distributions have been determined at 2, 6, 50, and 82 percent of the model semispan. This procedure is felt to be justified by the fact that the pressures at the two outboard orifice planes were unaffected by the change in end-plate height. The variation of pressure observed at the inboard orifice plane with end-plate position is interpreted as equivalent to the variation of pressure with spanwise position near the root of a wing with fixed end plate.

The test Mach numbers were determined from an average of the indications of two static-pressure tubes located 8 inches inboard and outboard of the model at the height of the particular spanwise station undergoing test. Each static-pressure tube was provided with two sets of static-pressure orifices which were set to bracket the airfoil chord at each station.

The tests consisted of a series of dives during each of which the Mach number was held constant for about 12 seconds while the model angle of attack was varied. The range of Mach number from 0.7 to 1.1 was covered in this manner in eight steps. At each step, continuous records were taken on standard NACA recording instruments of the model pressures and angle of attack, angle of flow at the reference vane, test section static pressure, airplane impact pressure, and atmospheric pressure and temperature. The model angle of attack was varied continuously between the limits -1° and 4° by a motor-driven cam at a rate of about 1° per second.

REPRODUCIBILITY OF DATA

The method used in transferring pressures from the orifices to the recording equipment limited the number of pressures which could be recorded simultaneously to 14. Because of this limitation, pressures were measured at alternate orifices on each surface of the model wing, so that two flights were required to complete a series of measurements at any given spanwise position. At Mach numbers below about 0.9 the data obtained during successive flights were in good agreement at all spanwise positions. At Mach numbers above 0.9, however, considerable scatter of the data was noted, particularly at the 82-percent-semispan position. Figure 5 has been prepared to show the magnitude of the scatter of the pressure data for the conditions most critical from the standpoint of repeatability. The individual chordwise pressure points are shown for several flights at each measuring station for Mach numbers between 0.9 and 1.1.

There has also been some evidence of an inaccuracy in the determination of the absolute magnitude of the angle of attack. Results to be

introduced in the section "Comparison with Force Tests" show that the section angle of zero lift varied in an apparently random manner along the span by as much as ±0.5°. This variation in the angle of zero lift is felt to be indicative of the general level of accuracy of the angle-of-attack measurement. Such errors in angle of attack may have been introduced by small errors arising in the positioning of the model on the wing-flow test panel from flight to flight. The scatter of the pressure data shown in figure 5 may have resulted, at least in part, from such errors in the angle of attack. It is emphasized, however, that the inaccuracy in the angle of attack is restricted to an error in absolute magnitude; changes in angle of attack measured on any one flight are considered to be accurate.

RESULTS AND DISCUSSION

Pressure Distributions

From faired curves of the pressure at each orifice as a function of Mach number and angle of attack for each of the spanwise positions investigated (2, 6, 50, and 82 percent semispan), points were taken off at angles of -1°, 0°, 2°, and 4° and at Mach numbers of 0.70, 0.80, 0.90, 0.95, 1.00, 1.05, and 1.10. The pressure distributions so obtained are shown in figures 6(a) to 6(g). The pressure distributions in figure 6 are grouped for equal values of the local Mach number at the different spanwise positions and do not correspond to a given instant of time. If, for example, the Mach number at 2 percent semispan was 0.70, the Mach number at 82 percent semispan would be about 0.67 at the same instant because of the decrease in Mach number with distance above the airplane wing surface. The measurement of pressure at the 6-percent-semispan position was obtained from the single test in which the end plate was lowered to 1/16 inch above the wing-flow cover plate. The pressure distributions at the 2-percent-semispan and 6-percent-semispan positions may be affected somewhat by the boundary layer from the airplane wing and by disturbances arising from the flow about the end plate.

A few of the salient features of the flow about sweptback wings can be seen immediately from the pressure distributions in figure 6 without resort to the integrated values of lift, drag, and moment coefficient. It is seen that at the root the leading-edge negative-pressure peaks are very small as compared with those observed on straight wings. However, pressure peaks near the leading edge develop rapidly with increasing spanwise position. As the Mach number is increased from 0.70 to 1.10, it is seen that the leading-edge pressure peaks progressively disappear at the more outboard stations.

Concomitant with the variation of the leading-edge peak pressure, the entire region of negative pressure on both the upper and lower surfaces of the airfoil shifts forward with increasing spanwise position and shifts rearward with increasing Mach number. These changes in shape of the pressure distributions reflect important variations of the section pressure-drag coefficient and center of pressure with spanwise position and Mach number. Examination of figure 6(a) for $M_l = 0.70$ indicates that the pressure drag, initially high at the center sections, decreases rapidly along the span. It will be shown that the pressure drag actually becomes negative near the tip under some conditions. The reduction of the peak negative pressure near the leading edge and the rearward shift of the negative-pressure region are indications that the pressure drag increases at all spanwise stations at the higher Mach numbers. It can be seen immediately from figure 6 that the center of pressure moves forward with increasing spanwise position at all Mach numbers, and moves rearward at all spanwise positions with increasing Mach number.

Integrated Forces and Moments

The spanwise lift, drag, and moment distributions given in subsequent sections represent the forces occurring over the airfoil at a given time and average Mach number (midspan Mach number) rather than at the same local Mach number for each section. The coefficients are obtained by expressing the forces and moments obtained from the pressure distributions in terms of the average dynamic pressure at the position of the model. The relations between the average and local Mach numbers are given in figure 7. The variation in Mach number from root to tip is of the order of that caused by the presence of a slender fuselage.

Lift characteristics.- The variation of section lift coefficient is shown as a function of average Mach number in figure 8 for each of the four spanwise stations. The variation of section lift-curve slope along the semispan is shown in figure 9 for several Mach numbers from 0.75 to 1.075. The relative spanwise lift distributions c_l/C_L for the same Mach numbers are shown in figure 10 and were calculated from the section lift-curve slopes of figure 9. The lift distributions show little change between the Mach numbers of 0.75 and 0.90 (fig. 10(a)). As the Mach number is increased from 0.90 to 1.00 (fig. 10(b)), a relative loss in lift occurs over the outboard sections of the wing and a relative increase in lift over the midsemispan sections. At the Mach number of 1.00, a small relative loss in lift is also evidenced near the wing root. With a further increase in Mach number from 1.00 to 1.075 (fig. 10(c)) the situation is reversed. The outboard sections of the wing show relative increases in lift while the more inboard sections show relative losses

in lift. The lift distribution for the Mach number of 1.075 is almost uniform across the wing semispan.

The experimental lift distribution for a Mach number of 0.75 is compared in figure 11 with the theoretical distribution calculated by the method of reference 4. The experimental and theoretical lift distributions are seen to agree closely except very near the root where the experimental distribution peaks sharply. This local disagreement between theory and experiment may result either from a slight misalinement of the end plate or from the effect of the airplane-wing boundary layer.

The lateral position of the center of pressure expressed as a fraction of the wing semispan is shown as a function of average Mach number in figure 12. The variation of lateral position of the center of pressure with average Mach number merely reflects the changes in the spanwise lift distribution discussed in connection with figure 10. The lateral center of pressure was constant at 47 percent semispan for Mach numbers between 0.75 and 0.90, moved inboard slightly at a Mach number of 1.0, and moved outboard to 50 percent semispan at a Mach number of 1.075. The theoretical center of pressure of this wing was calculated to be at 48 percent semispan at low Mach numbers.

Drag characteristics.- The variation of section pressure-drag coefficient along the semispan of the model wing is shown in figure 13 for several average Mach numbers between 0.75 and 1.075 and for angles of attack from -1° to 4°. For all Mach numbers and at all angles of attack the section pressure-drag coefficient is seen to be a maximum at the wing root and to decrease along the semispan. For Mach numbers less than 1.00 the pressure drag was negative near the wing tip. In general, as the Mach number was increased from 0.75 to 1.00 there was an increase in the pressure drag at the wing root and an increase in the negative pressure drag near the wing tip. It will be shown that at least for angles of attack up to 2° the total pressure drag of the wing remained very nearly constant. As the Mach number was increased from 1.00 to 1.075 (fig. 13(b)) the pressure-drag coefficient remained nearly constant near the root but increased rapidly at the more outboard stations. The over-all pressure drag of the wing, of course, increased rapidly as the Mach number exceeded 1.00.

The spanwise pressure-drag distributions measured at an angle of attack of -1° (near zero lift) and Mach numbers of 0.90 and 1.05 are compared in figure 14 with theoretical zero-lift pressure-drag distributions calculated by the methods of references 5 and 6. The theoretical wing had the same plan form and thickness ratio as the experimental wing but was assumed to have parabolic-arc airfoil sections. At the Mach number of 0.90 (fig. 14(a)) the theoretical and experimental section

pressure-drag coefficients show similar variations along the span and are roughly of the same magnitude. At the Mach number of 1.05 (fig. 14(b)) the theoretical and experimental values were in agreement only at the root; over the outboard sections of the wing the experimental pressure-drag coefficient was considerably greater than the theoretical value. The integrated theoretical and experimental values of the wing pressure-drag coefficient at the Mach number of 1.05 are 0.0068 and 0.0147, respectively.

The over-all pressure-drag coefficient C_D of the wing is shown in figure 15 as a function of average Mach number for several angles of attack. It is seen that for the angles of attack tested the values of C_D are fairly constant at Mach numbers below about 0.95 but increase rapidly at higher Mach numbers. The value of C_D of 0.002 measured at the angles of attack of -1° and 0° (essentially zero lift) at the lower Mach numbers is about that to be expected as the result of separation at the low test Reynolds number. The increase in C_D above the base value of 0.002 at 2° angle of attack is about that to be expected from the induced drag due to the production of lift. However, at 4° angle of attack the increase in C_D is greater by about 0.004 than can be accounted for by the induced drag, and must result in part from an increase in profile drag.

Pitching-moment characteristics.- The variation of the section pitching moment with position along the semispan of the wing is shown in figure 16 for a series of Mach numbers and for angles of attack from -1° to 4°. The section pitching-moment coefficients as presented in figure 16 have been calculated about an axis normal to the plane of symmetry and passing through the center of area of the semispan wing plan form. The over-all wing pitching-moment characteristics have been obtained from the data of figure 16 and are presented as the variation of $\frac{dC_m}{dC_L}$ with average Mach number in figure 17. The parameter $\frac{dC_m}{dC_L}$ represents the longitudinal position of the wing aerodynamic center ahead of the center of area of the plan form expressed as a fraction of the streamwise chord.

Comparison with force tests.- Some of the results obtained from the pressure measurements of this study are compared in figure 18 with the results of wing-flow force-test measurements obtained on an identical wing model (reference 7). Inasmuch as the coefficients of the force tests were based on the values of the dynamic pressure and Mach number at the wing root, the coefficients obtained from the pressure measurements are also expressed in these terms in figure 18.

The angles of zero lift measured for each of the 4 spanwise stations are seen to be in general agreement with the angle of zero lift obtained from the force tests (fig. 18(a)), although there is a variation in the pressure data of almost $\pm 0.5^{\circ}$ from station to station. Inasmuch as there is no reason to expect the angle of zero lift to vary along the span of the wing, at least at the lower Mach numbers, the variations which were obtained are assumed to be of a random nature. It is felt that such random variations could easily arise from small inaccuracies incurred in the positioning of the wing-flow model on the test panel from flight to flight. Although the absolute value of the angle of attack may be uncertain by almost as much as $\pm 0.5^{\circ}$, there is no reason to expect that changes in angle of attack were not measured accurately. Hence, the aerodynamic derivatives such as $\frac{dC_L}{d\alpha}$ and $\frac{dC_m}{dC_L}$ and the relative lift distributions, as computed, should be accurately determined.

In figures 18(b) and 18(c) it is seen that the values of $\frac{dC_L}{d\alpha}$ and $\frac{dC_m}{dC_L}$, respectively, determined from the pressure measurements and force tests are in substantial agreement.

In figure 18(d) a comparison is given of the variation of the total drag coefficient (pressure drag plus skin friction) near zero lift with Mach number as determined from the pressure measurements and the force tests of reference 7. The values of the zero-lift drag coefficients obtained from the two sources are in fair agreement. The values of total drag coefficient for the pressure measurements are the values of pressure-drag coefficient C_D for $\alpha = -1^{\circ}$ in figure 15 plus 0.006 to account for the skin-friction drag.

CONCLUDING REMARKS

Measurements of pressure have been made over a 45° sweptback semispan wing model of 3.5 aspect ratio with 2-inch-chord NACA 65-210 airfoil sections normal to the leading edge. The tests were conducted by the NACA wing-flow method at Mach numbers from about 0.7 to 1.1 and angles of attack from -1° to 4° at a nominal Reynolds number of 0.6×10^{6} based on the chord in the stream direction.

Little change in the spanwise lift distribution was found to occur at Mach numbers between 0.7 and 1.1. The spanwise center of load was always between 45 and 50 percent semispan.

The section pressure-drag coefficient was found to be a maximum at the wing root and to decrease along the span at all Mach numbers. At

a Mach number of 0.90 the experimental and theoretical section pressure-drag coefficients showed similar variations along the span and were roughly of the same magnitude. At a Mach number of 1.05 agreement between the experimental and theoretical section pressure-drag coefficients was obtained only near the wing root; at the more outboard stations the experimental drag coefficients were higher than the theoretical.

Comparison of the data of this investigation with previously published wing-flow force-test measurements showed good agreement for the slopes of the wing lift and pitching-moment curves and the zero-lift wing drag coefficient at all test Mach numbers ($M = 0.75$ to $M = 1.075$).

Langley Aeronautical Laboratory
National Advisory Committee for Aeronautics
Langley Field, Va.

REFERENCES

1. Lippisch, A., and Beuschausen, W.: Pressure Distribution Measurements at High Speed and Oblique Incidence of Flow. NACA TM 1115, 1947.

2. Frick, Charles W., and Boyd, John W.: Investigation at Supersonic Speed (M = 1.53) of the Pressure Distribution over a 63° Swept Airfoil of Biconvex Section at Zero Lift. NACA RM A8C22, 1948.

3. Boyd, John W., Katzen, Elliott D., and Frick, Charles W.: Investigation at Supersonic Speed (M = 1.53) of the Pressure Distribution over a 63° Swept Airfoil of Biconvex Section at Several Angles of Attack. NACA RM A8F22, 1948.

4. DeYoung, John: Theoretical Additional Span Loading Characteristics of Wings with Arbitrary Sweep, Aspect Ratio, and Taper Ratio. NACA TN 1491, 1947.

5. Jones, Robert T.: Subsonic Flow over Thin Oblique Airfoils at Zero Lift. NACA Rep. 902, 1948. (Formerly NACA TN 1340.)

6. Harmon, Sidney M., and Swanson, Margaret D.: Calculations of the Supersonic Wave Drag of Nonlifting Wings with Arbitrary Sweepback and Aspect Ratio. Wings Swept behind the Mach Lines. NACA TN 1319, 1947.

7. Zalovcik, John A., and Adams, Richard E.: Preliminary Tests at Transonic Speeds of a Model of a Constant-Chord Wing with a Sweepback of 45° and an NACA $65_{(112)}$-210, a = 1.0 Airfoil Section. NACA ACR L5J16a, 1945.

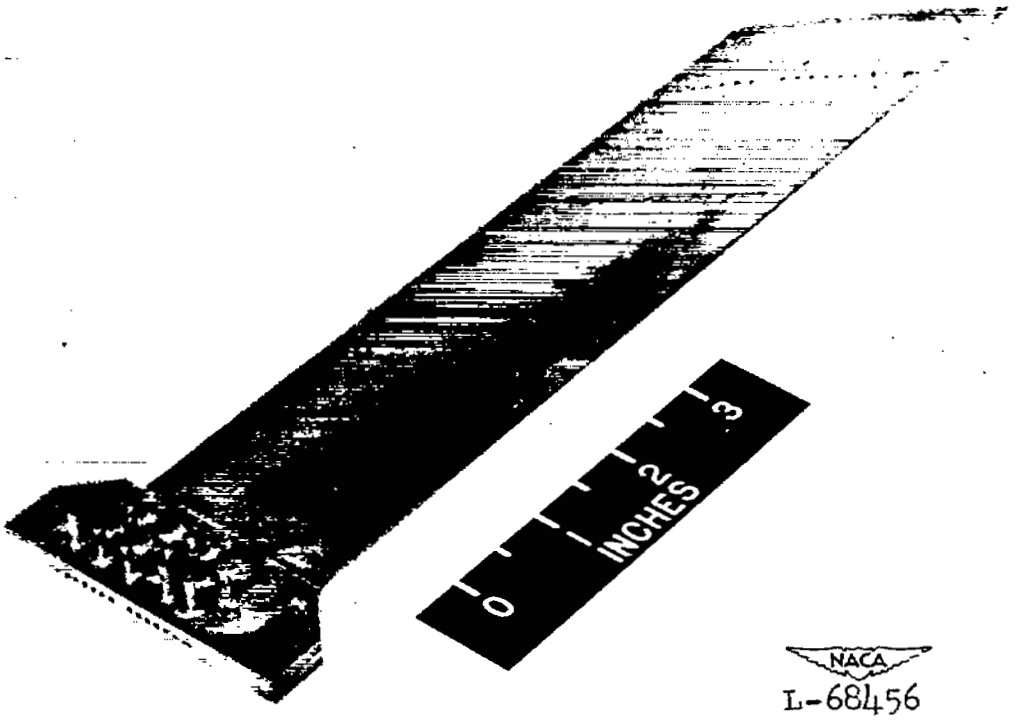

Figure 1.- NACA 65-210 airfoil model.

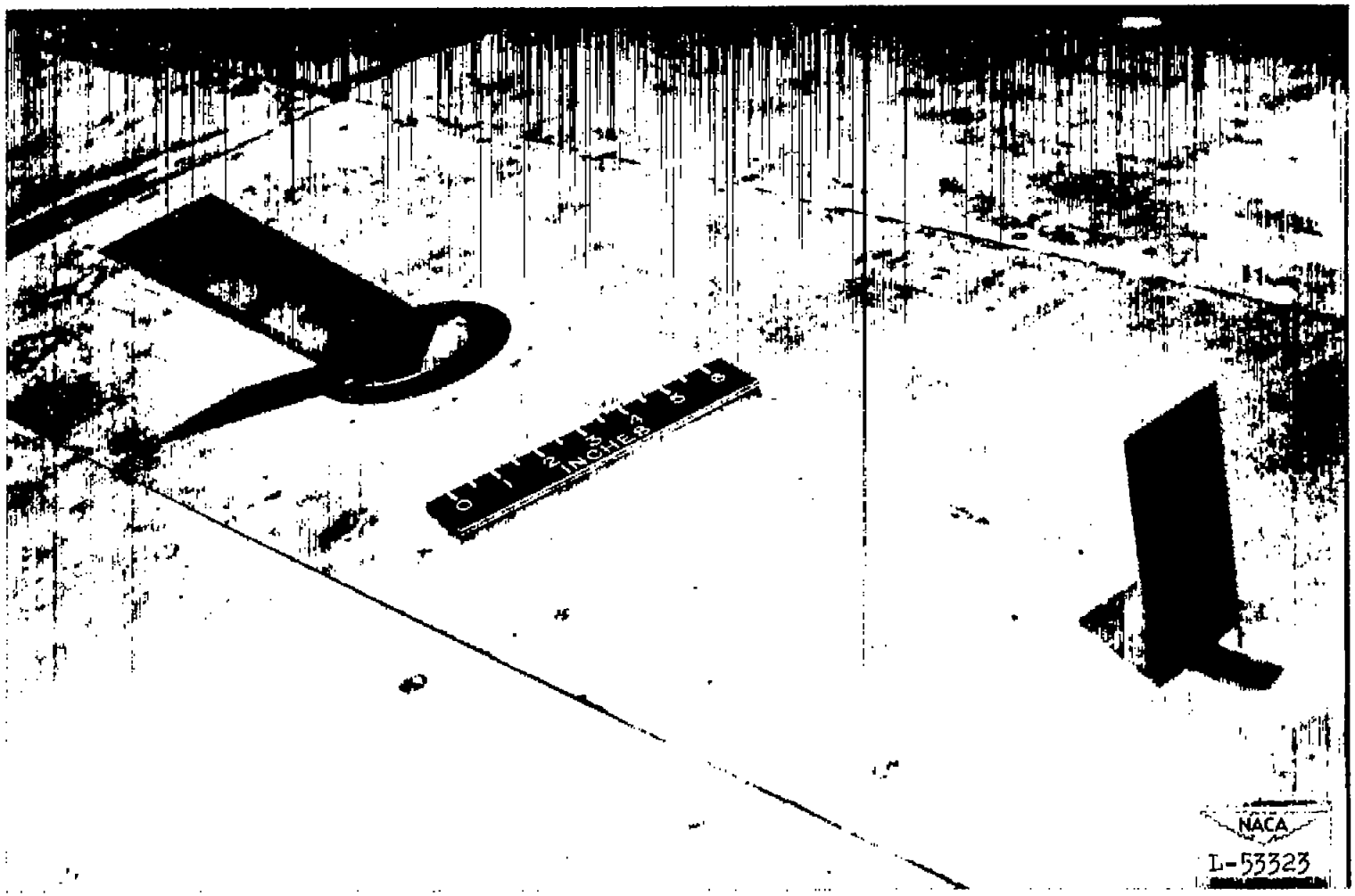

Figure 2.- Airfoil model mounted on airplane wing.

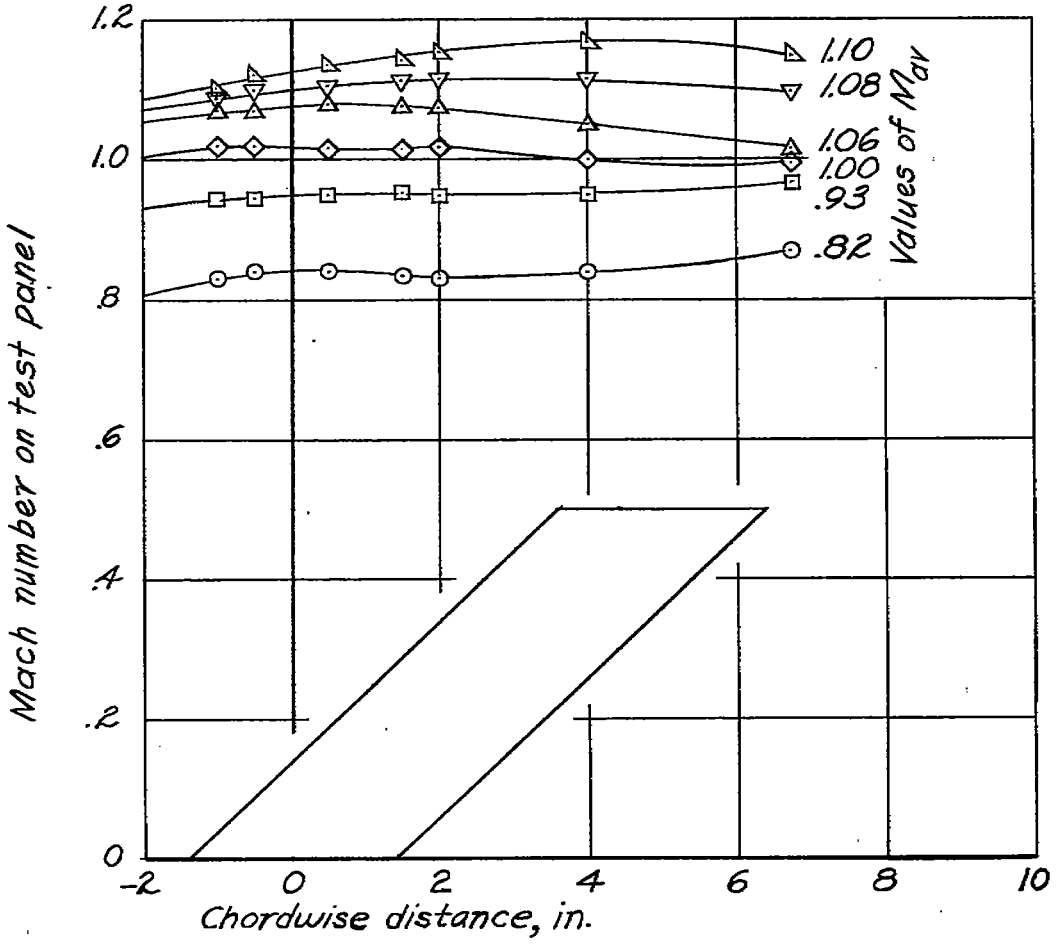

(a) Mach number distributions on test panel in region of model.

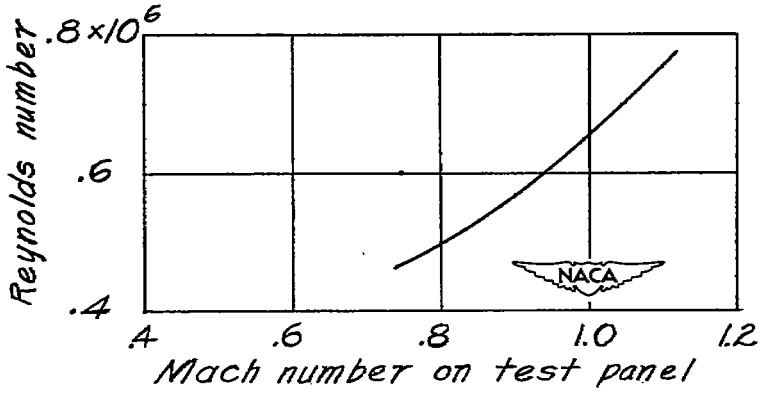

(b) Variation of Reynolds number with Mach number on test panel.

Figure 3.- Typical flow conditions.

Orifice locations

Orifice	$\frac{x}{c}$	Orifice	$\frac{x}{c}$
1 *	.03	9	.46
2	.06	10	.51
3	.11	11	.56
4	.16	12	.61
5	.21	13	.66
6	.26	14	.71
7	.31	15	.78
8	.36	16	.90

* Orifice on upper surface only.

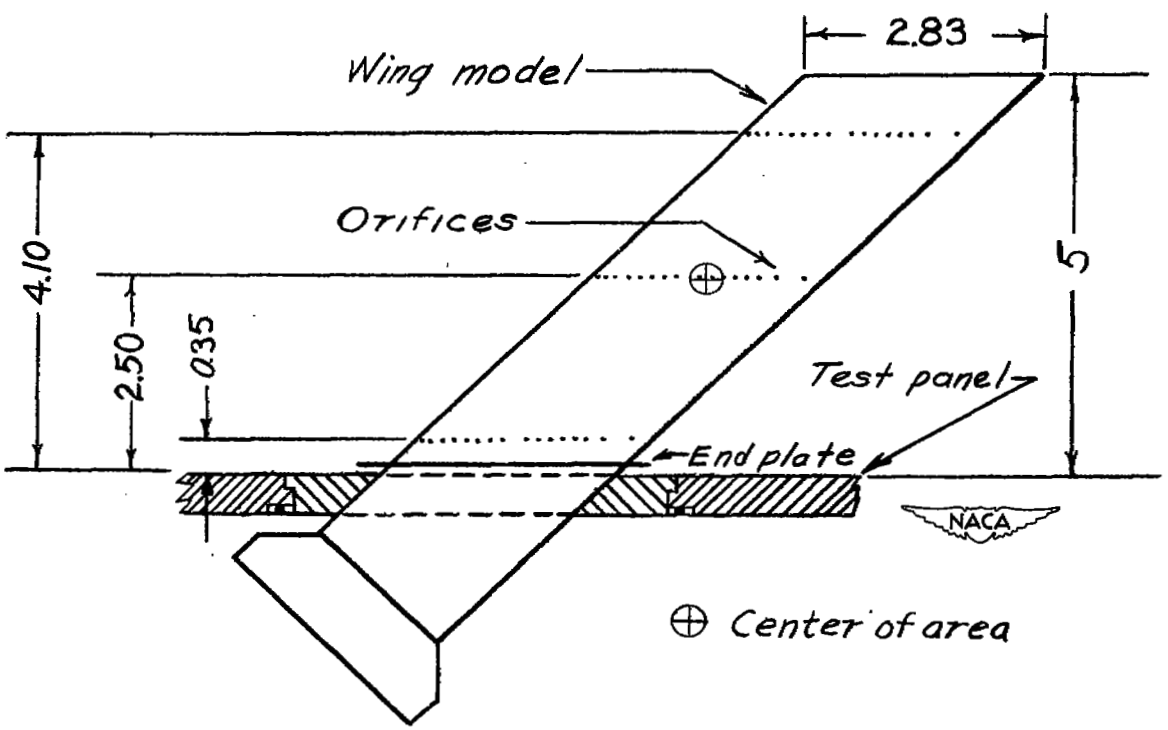

Figure 4.- Sketch of wing model mounted on test panel and table of orifice locations. All dimensions are in inches.

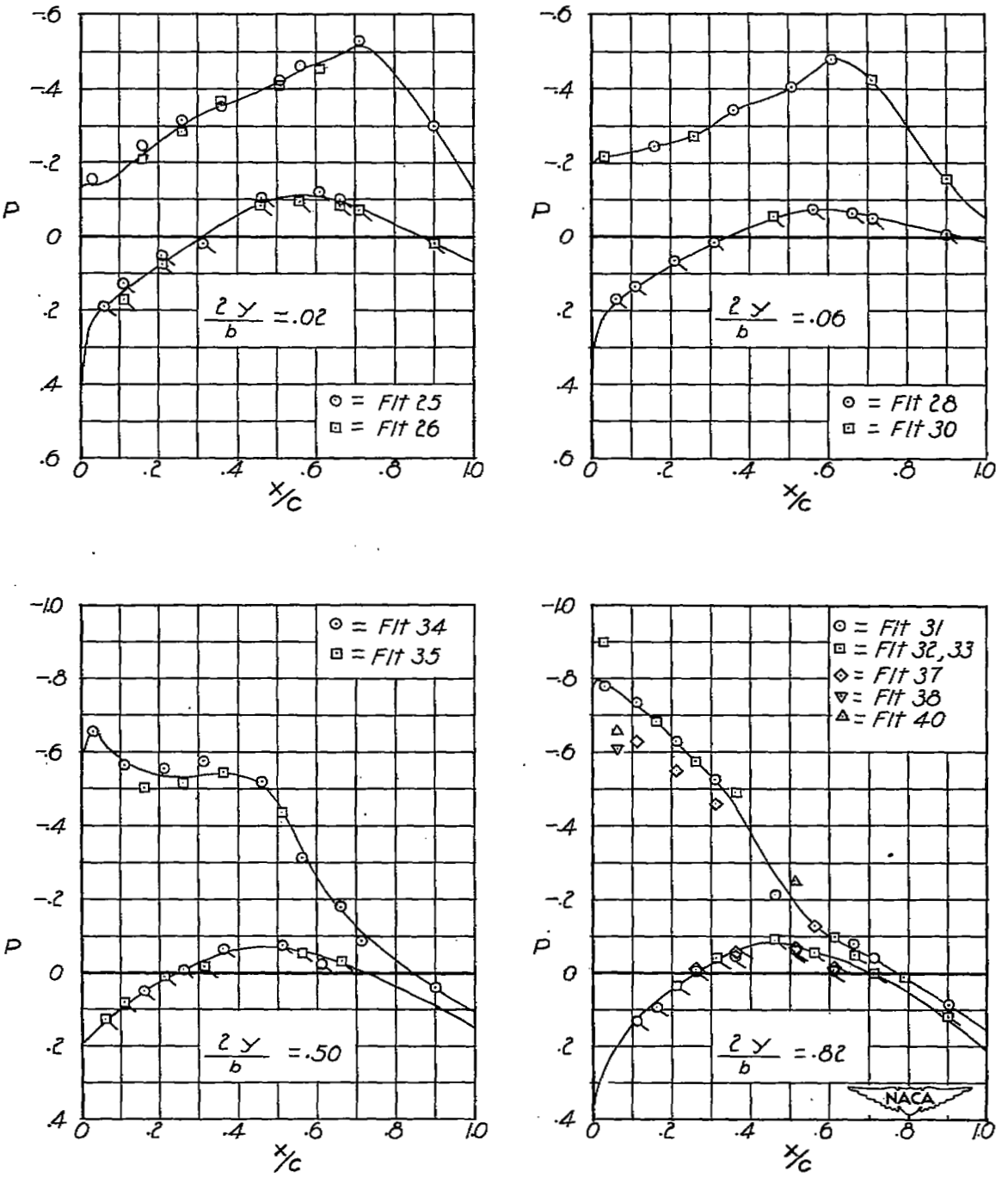

(a) $M_l = 0.9$. Flagged symbols denote lower surface.

Figure 5.- Chordwise pressure distributions over wing model showing reproducibility of data from flight to flight. $\alpha = 4^{\circ}$.

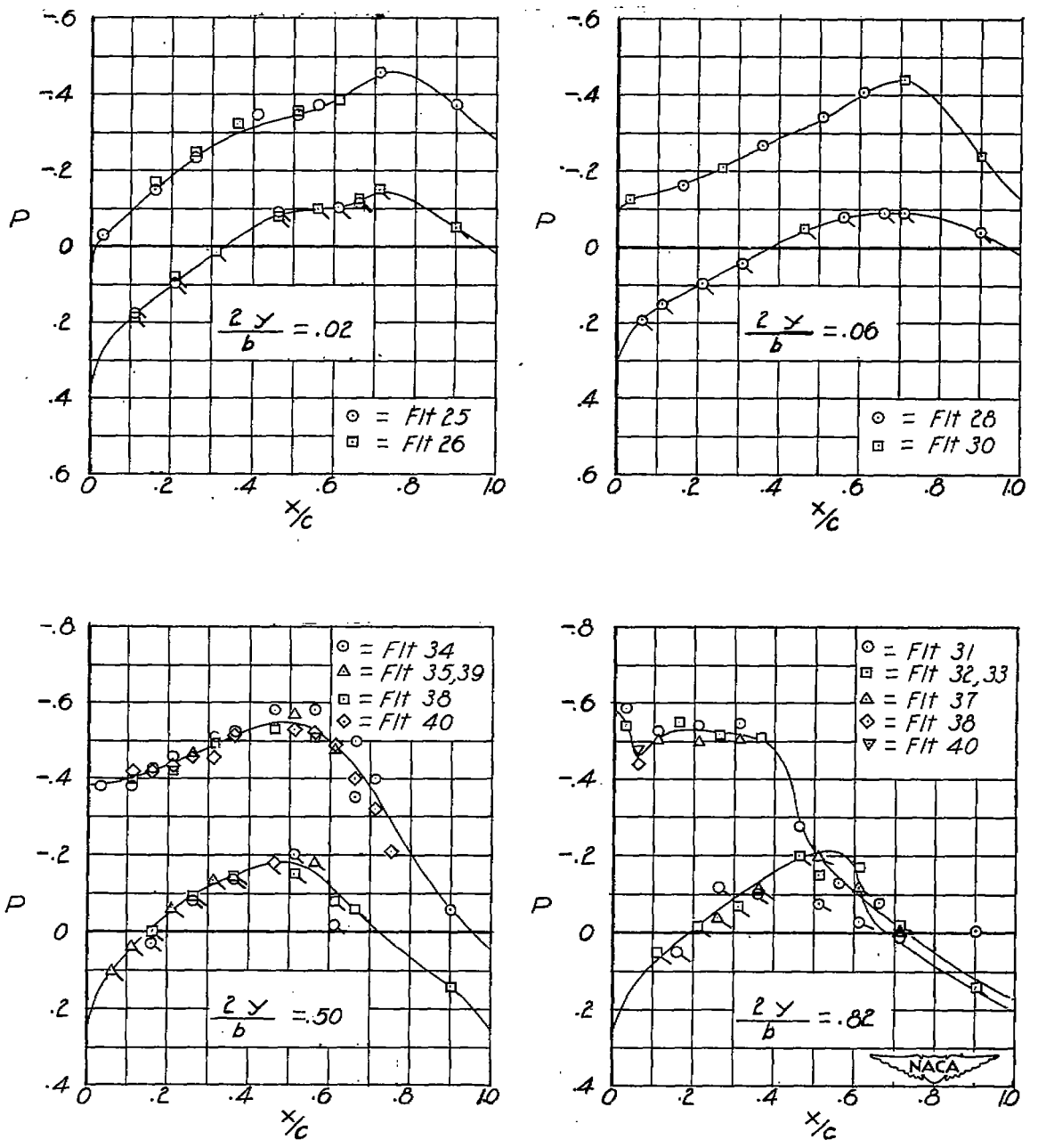

(b) M_l = 1.0. Flagged symbols denote lower surface.

Figure 5.- Continued.

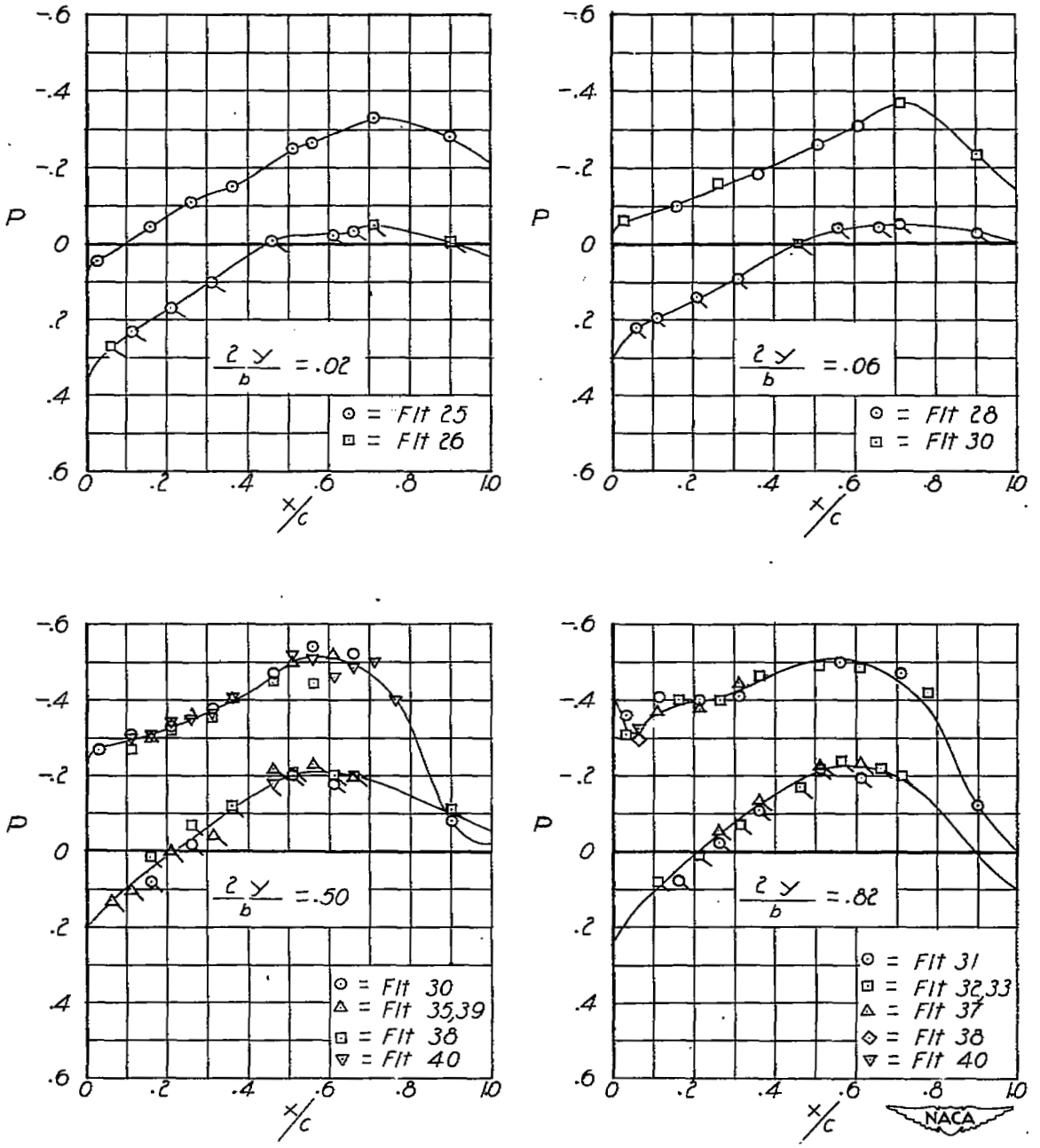

(c) M_l = 1.1. Flagged symbols denote lower surface.

Figure 5.- Concluded.

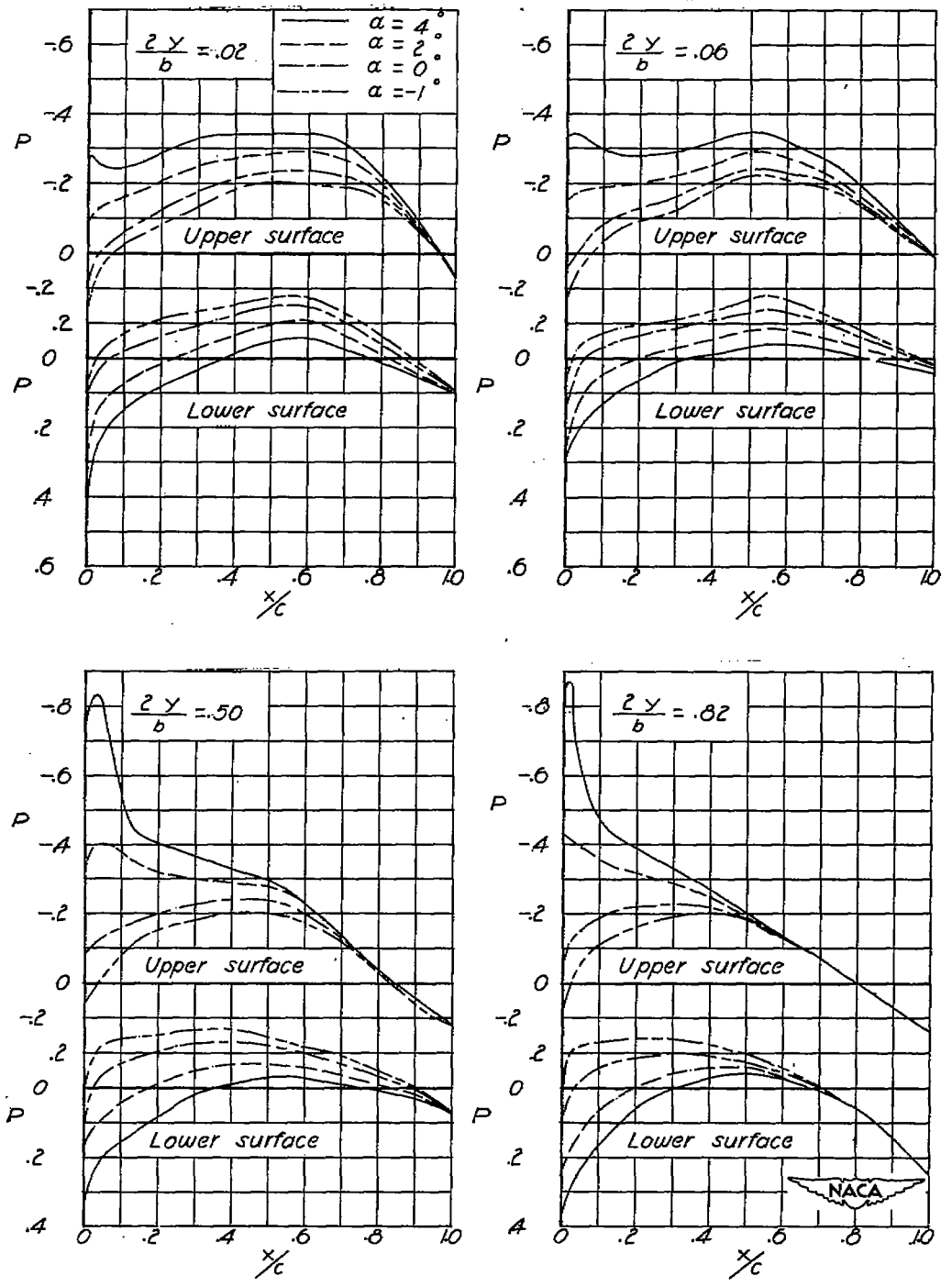

(a) $M_l = 0.70$.

Figure 6.- Chordwise pressure distributions at various spanwise positions for several Mach numbers.

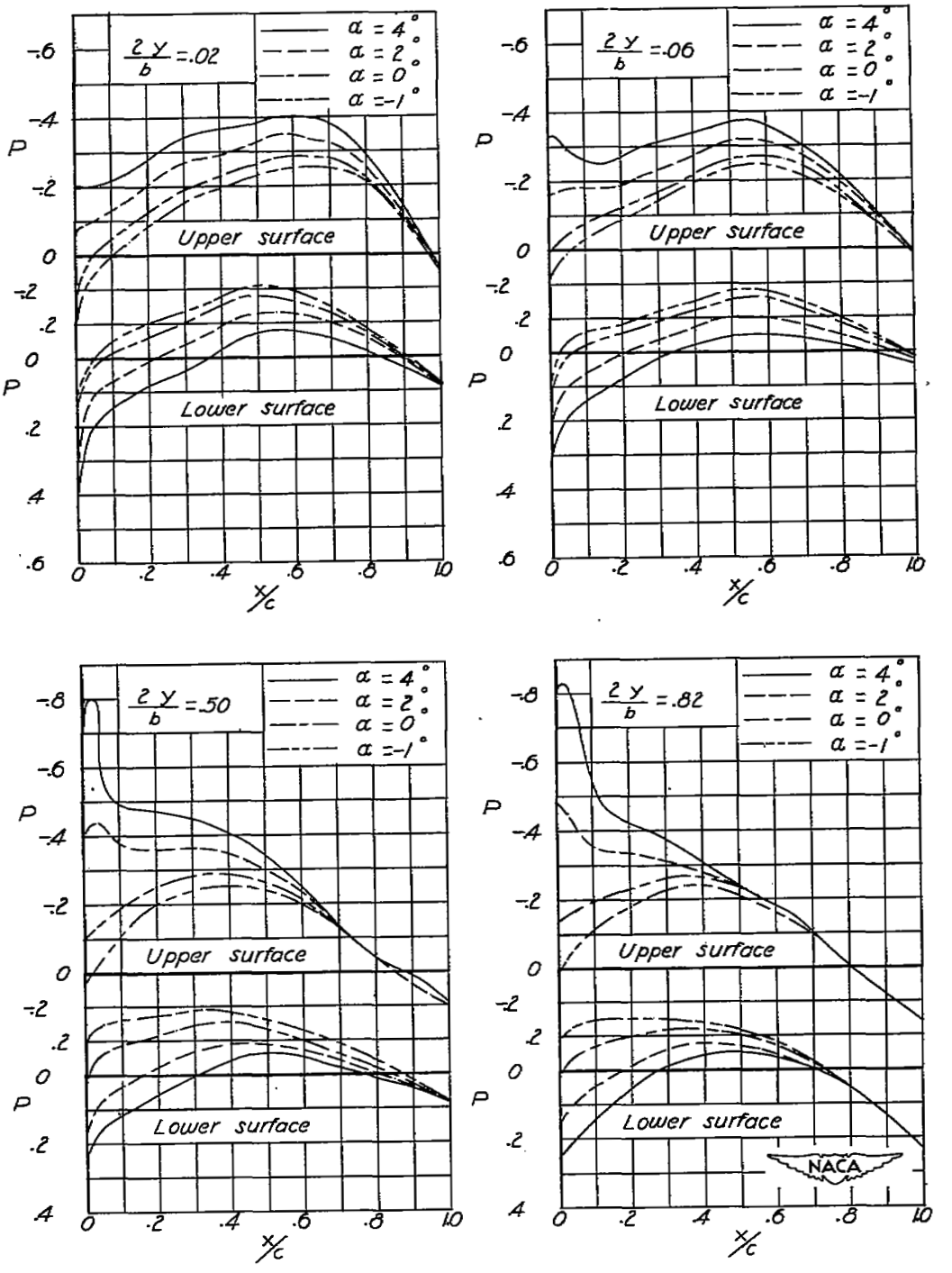

(b) $M_l = 0.80$.

Figure 6.- Continued.

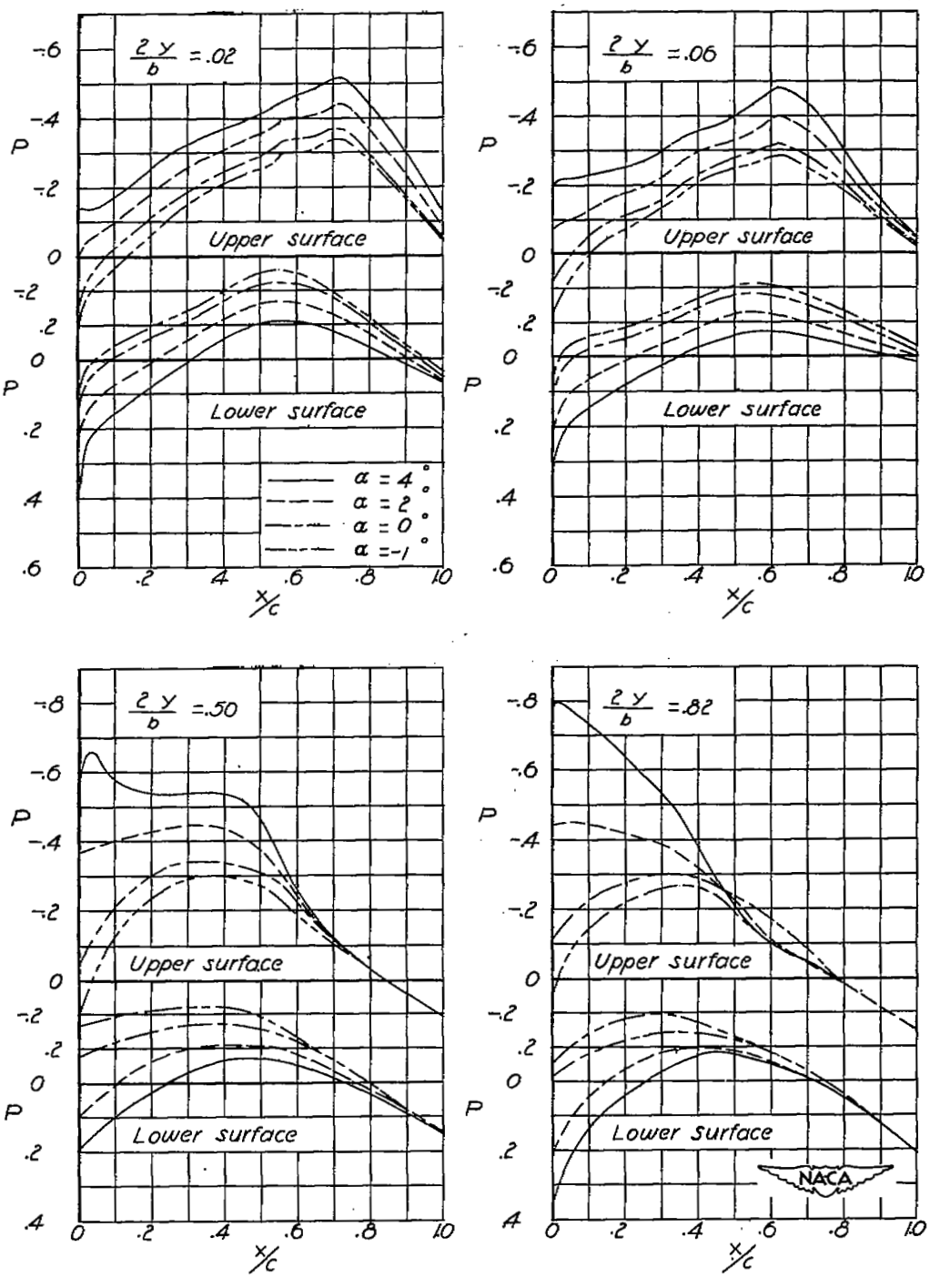

(c) $M_l = 0.90$.

Figure 6.- Continued.

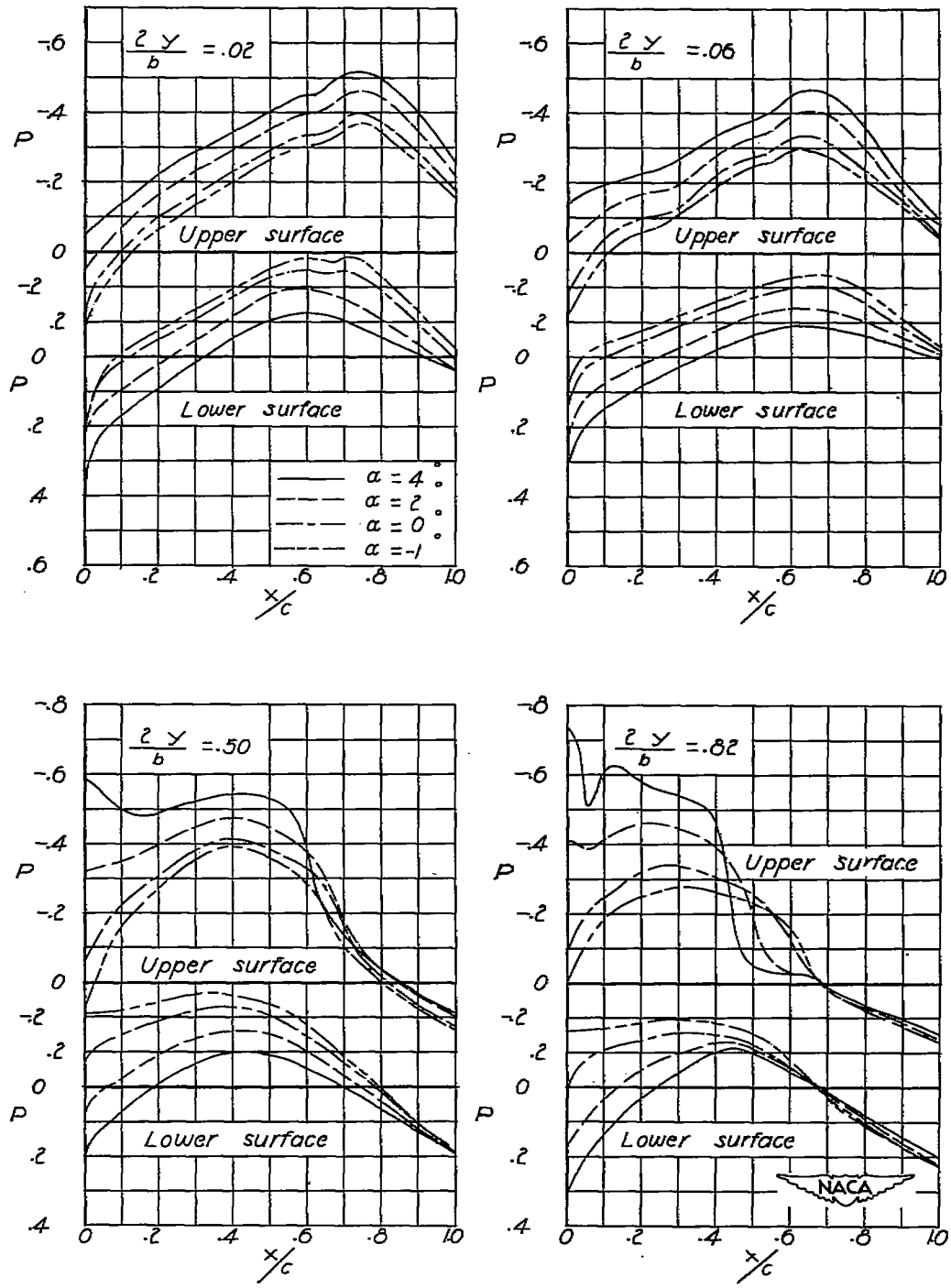

(d) $M_l = 0.95$.

Figure 6.- Continued.

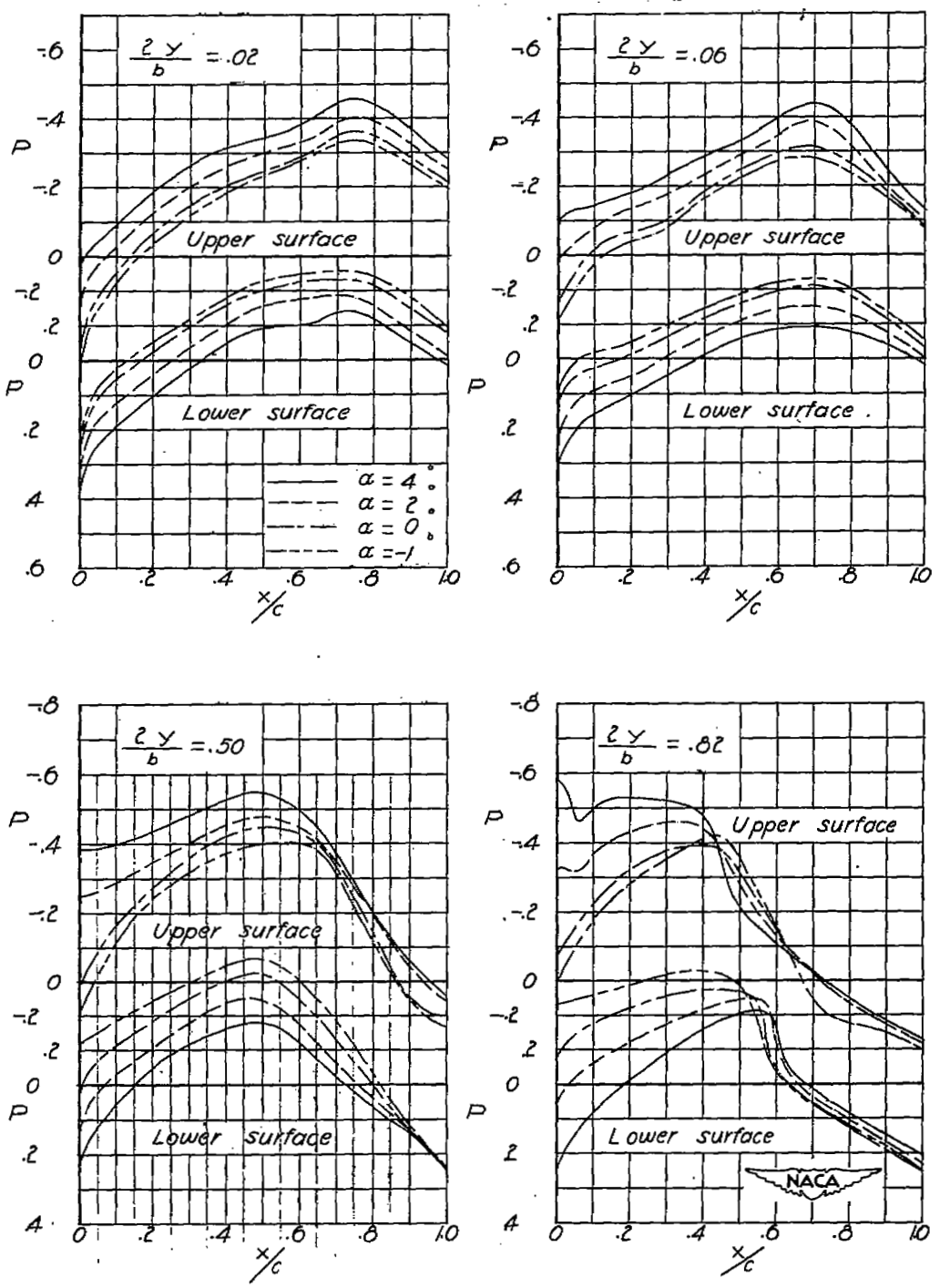

(e) $M_l = 1.00$.

Figure 6.- Continued.

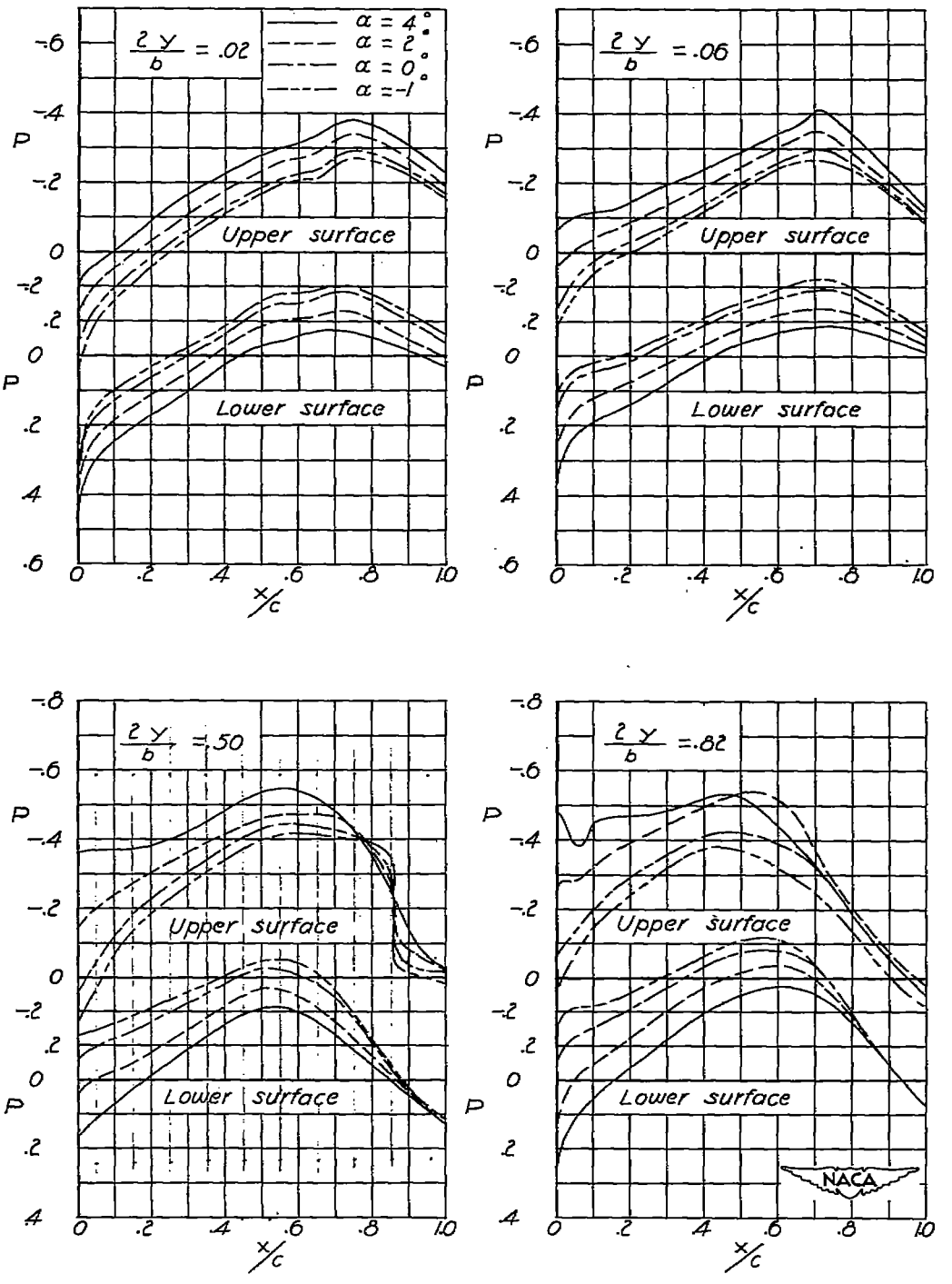

(f) $M_l = 1.05$.

Figure 6.- Continued.

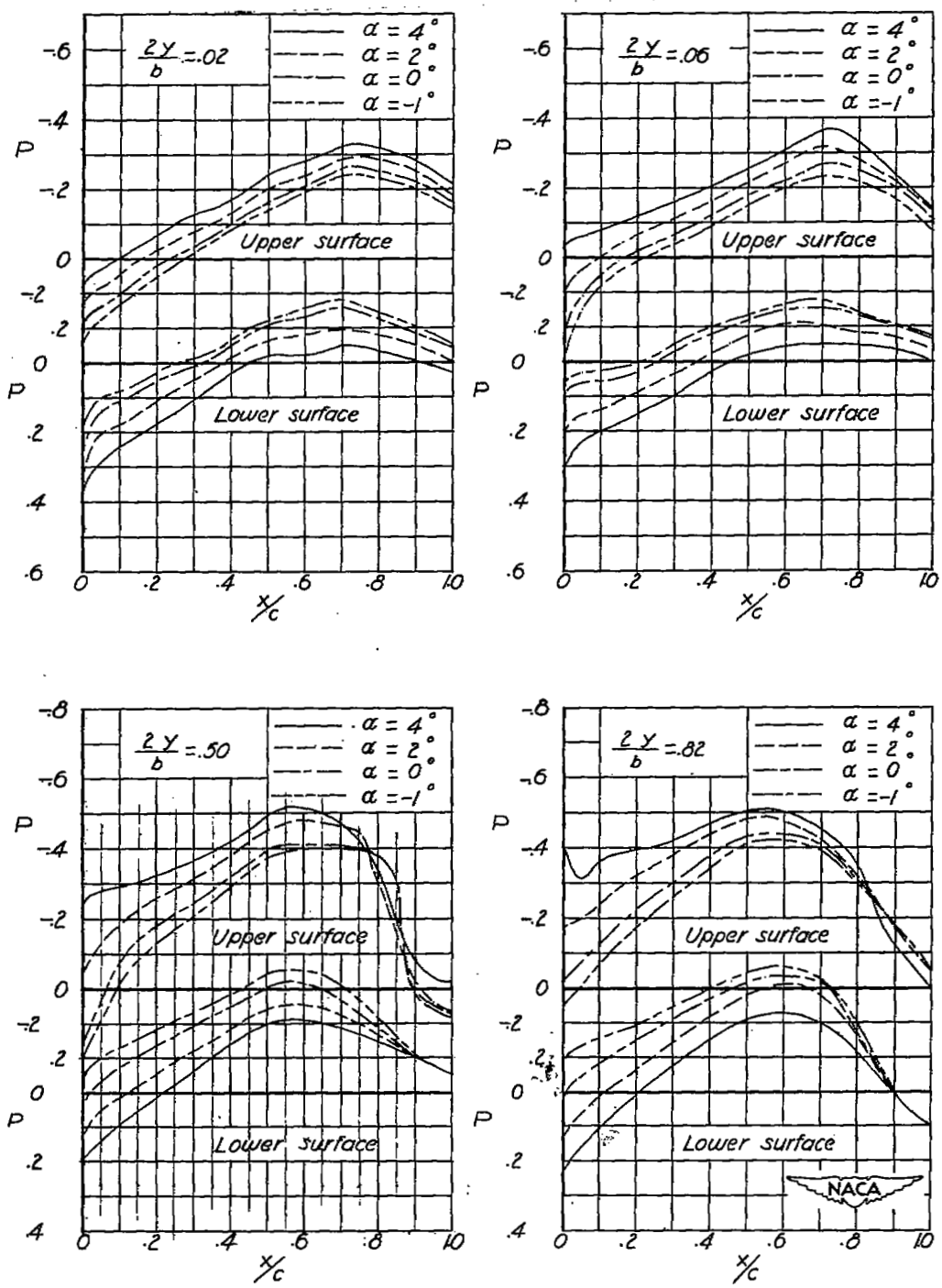

(g) $M_l = 1.10$.

Figure 6.- Concluded.

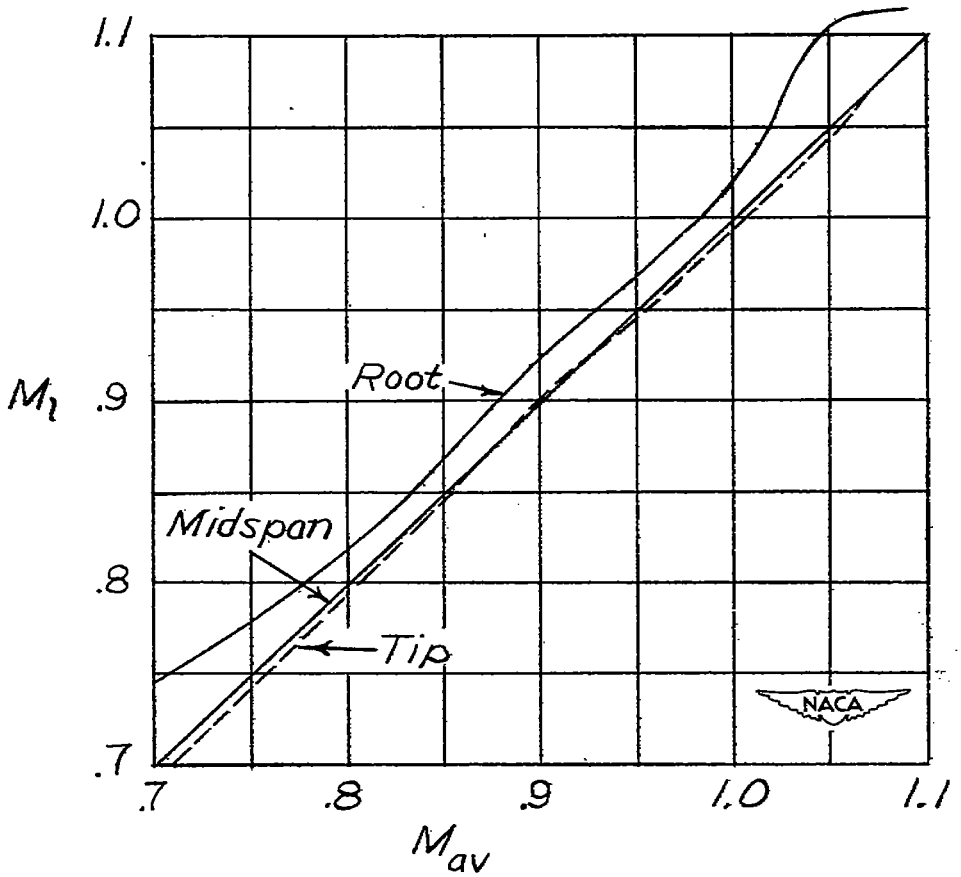

Figure 7.- Relation between the average Mach number and the local Mach number at each measuring station.

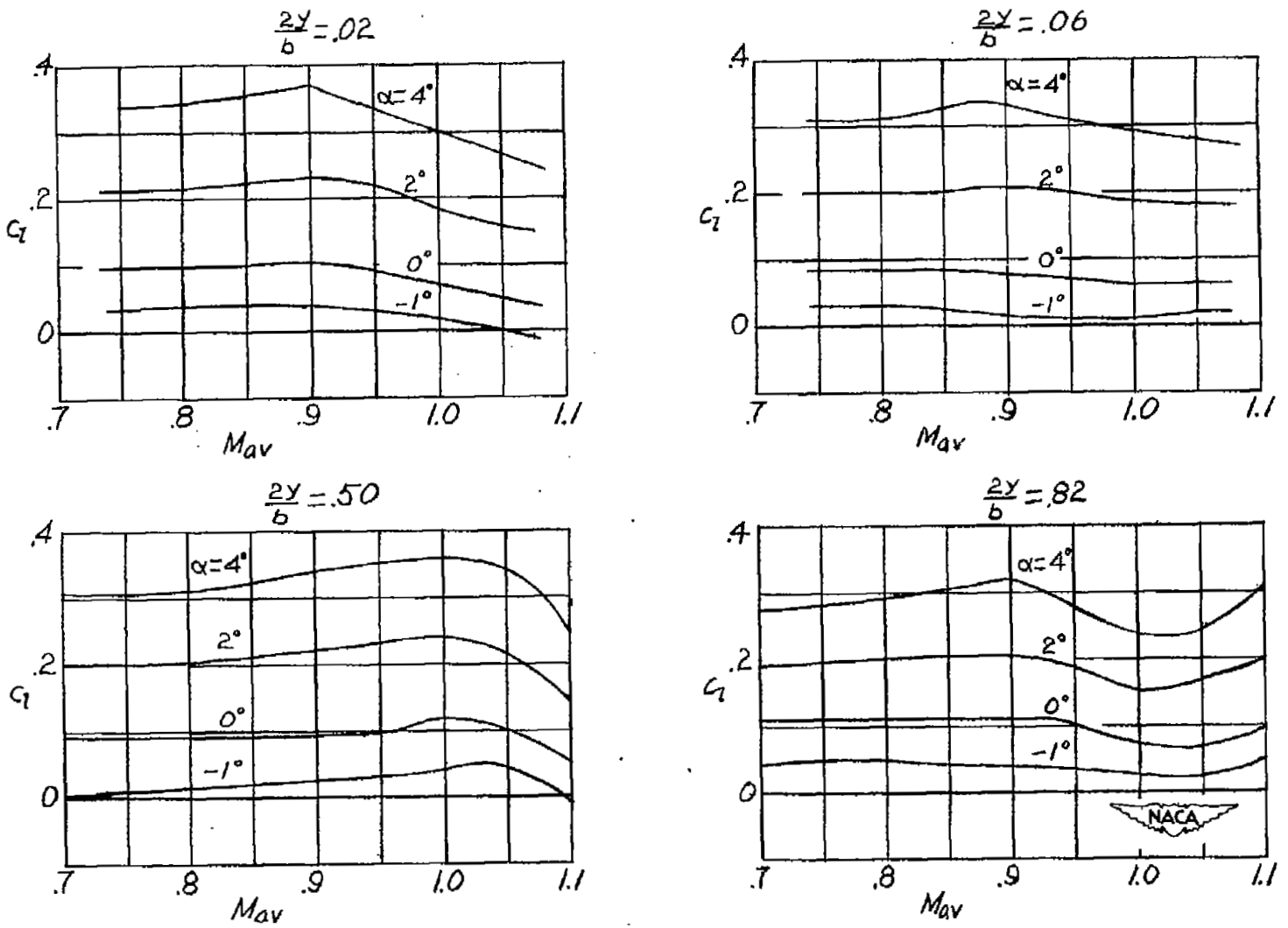

Figure 8.- Variation of section lift coefficient with average Mach number at selected angles of attack.

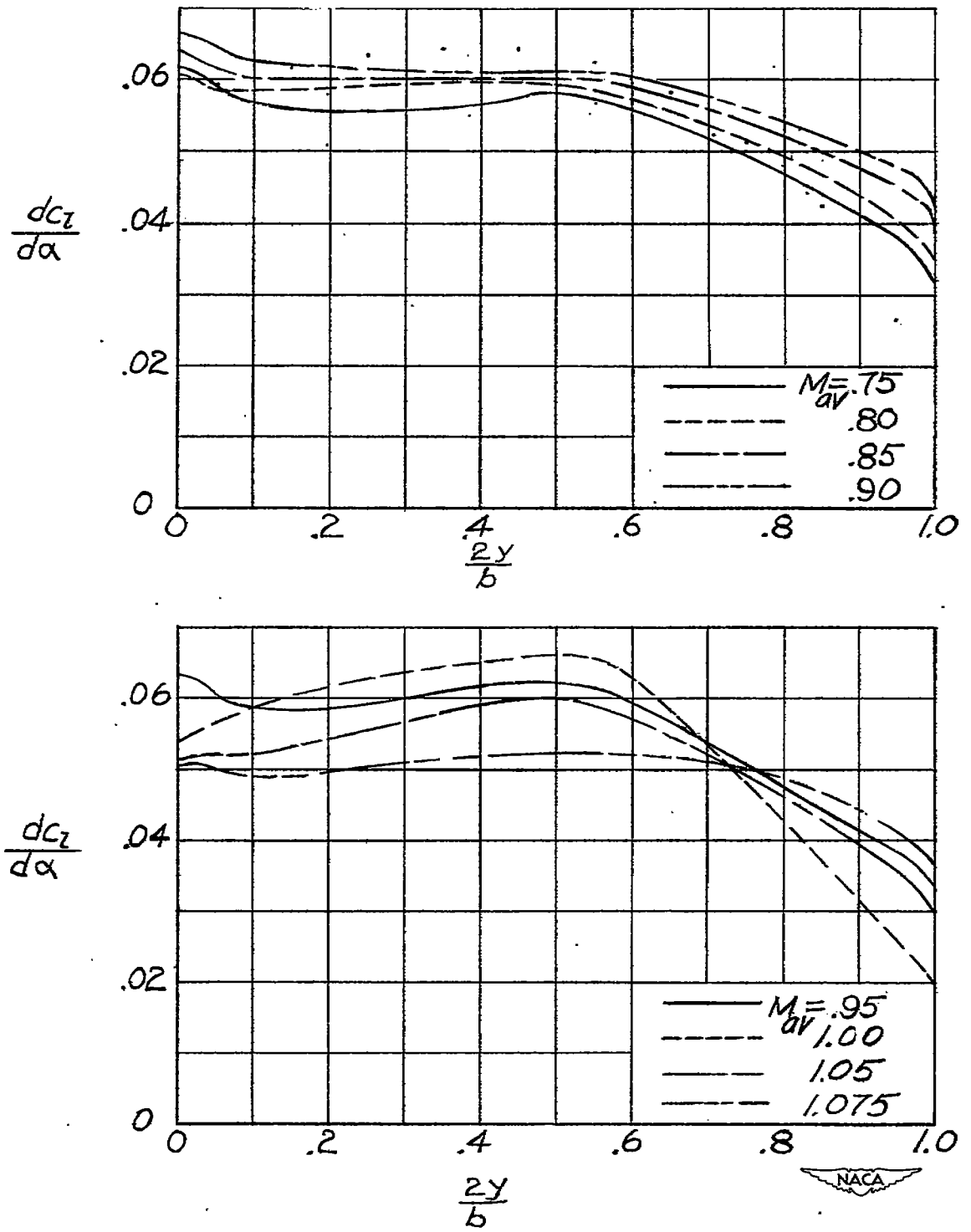

Figure 9.- Spanwise variation of section lift-curve slope for selected values of average Mach number.

[redacted]

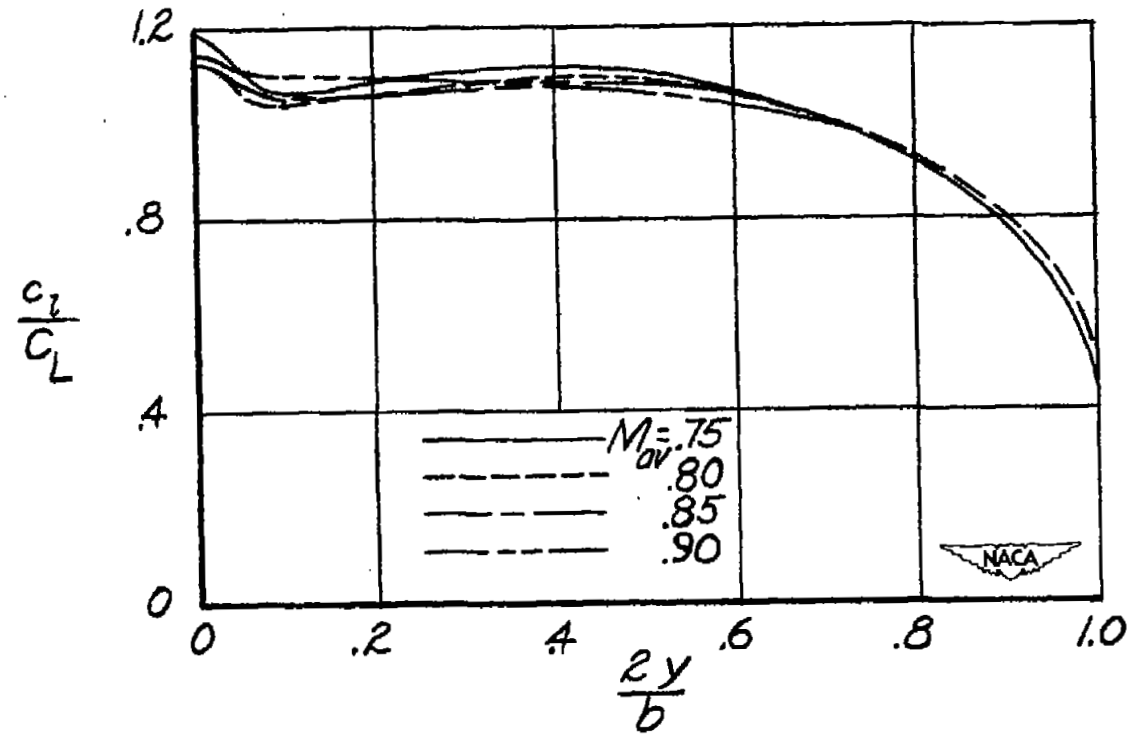

(a) M_{av} from 0.75 to 0.90.

Figure 10.- Relative spanwise lift distributions for several average Mach numbers.

[redacted]

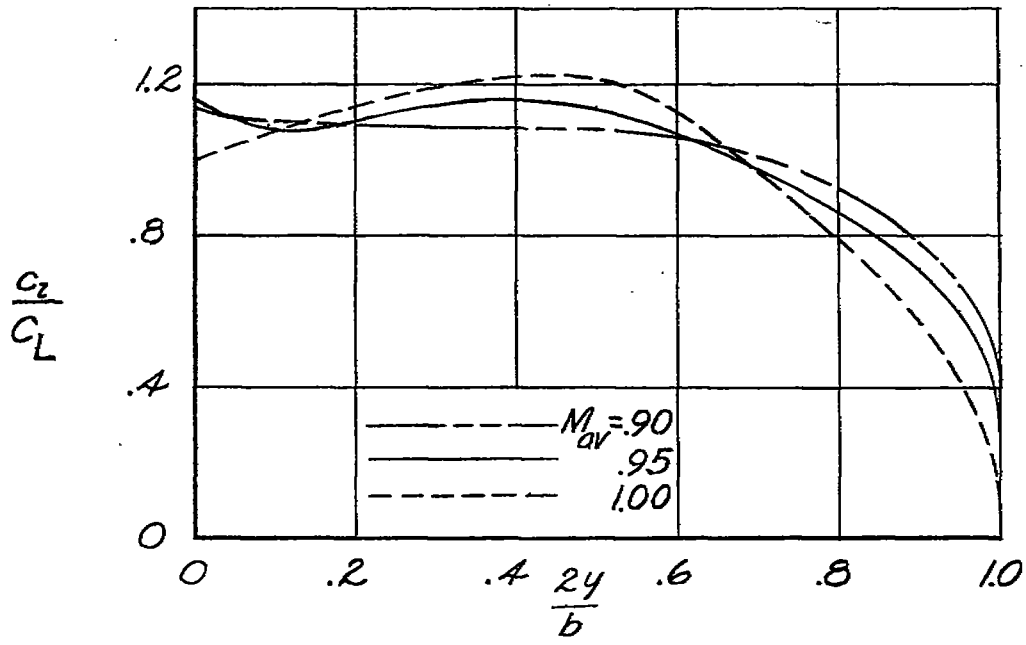

(b) M_{av} from 0.90 to 1.00.

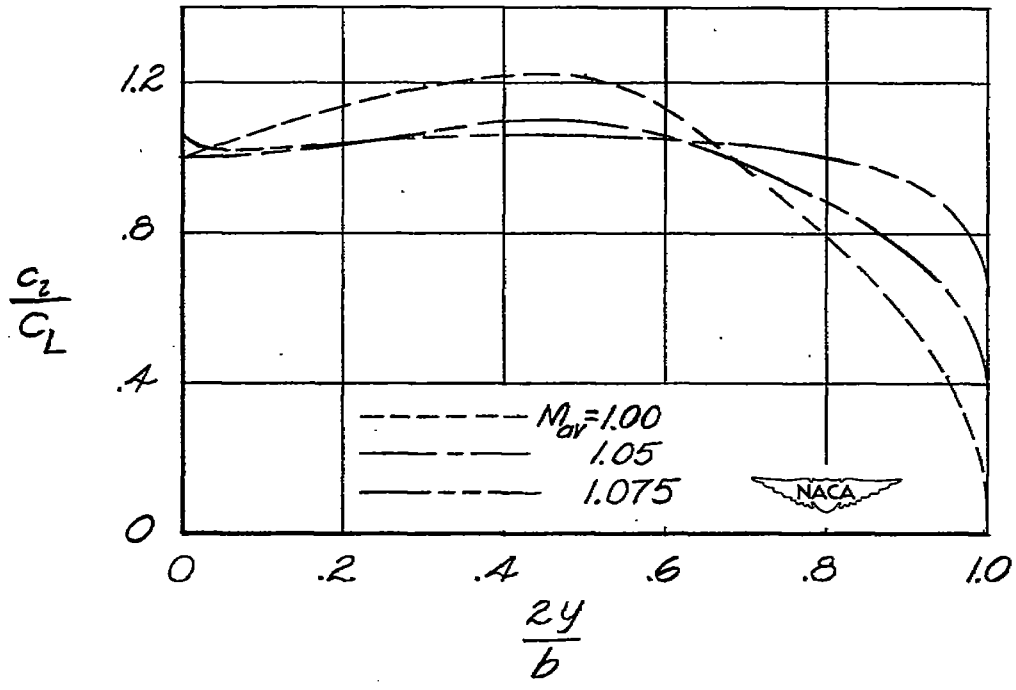

(c) M_{av} from 1.00 to 1.075.

Figure 10.- Concluded.

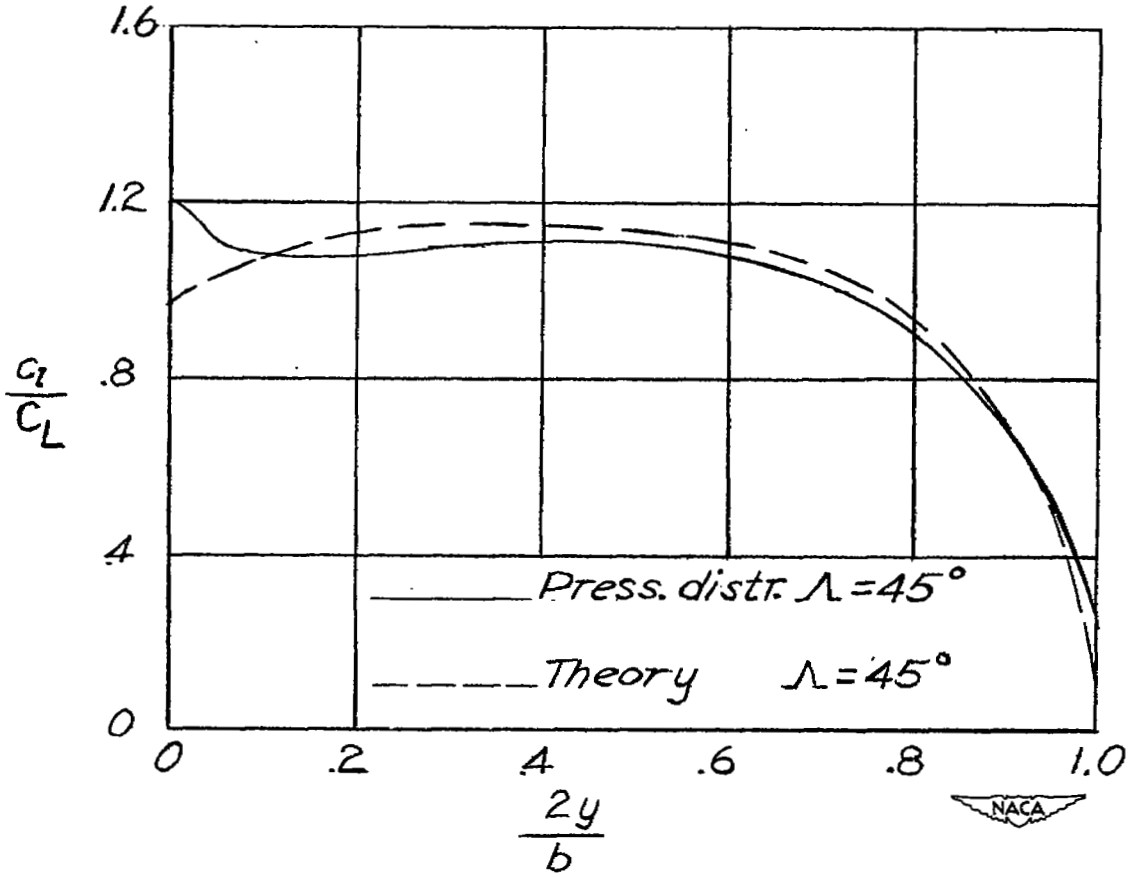

Figure 11.- Comparison of experimental and theoretical span load distributions for an average Mach number of 0.75.

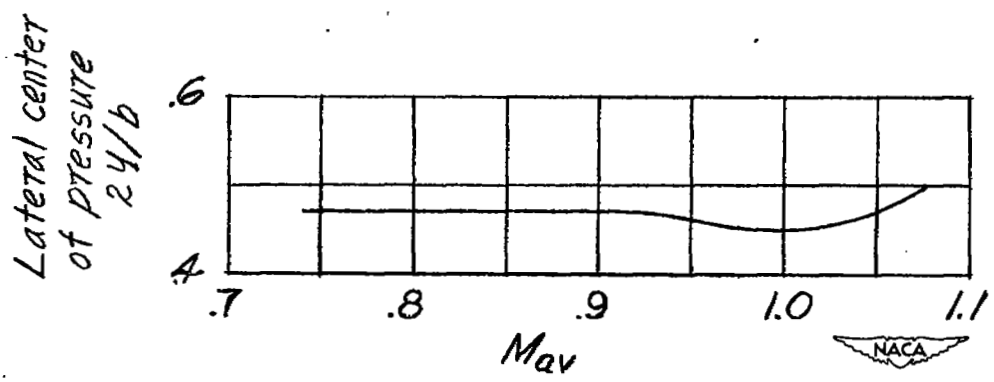

Figure 12.- Variation of the position of the lateral center of pressure with average Mach number.

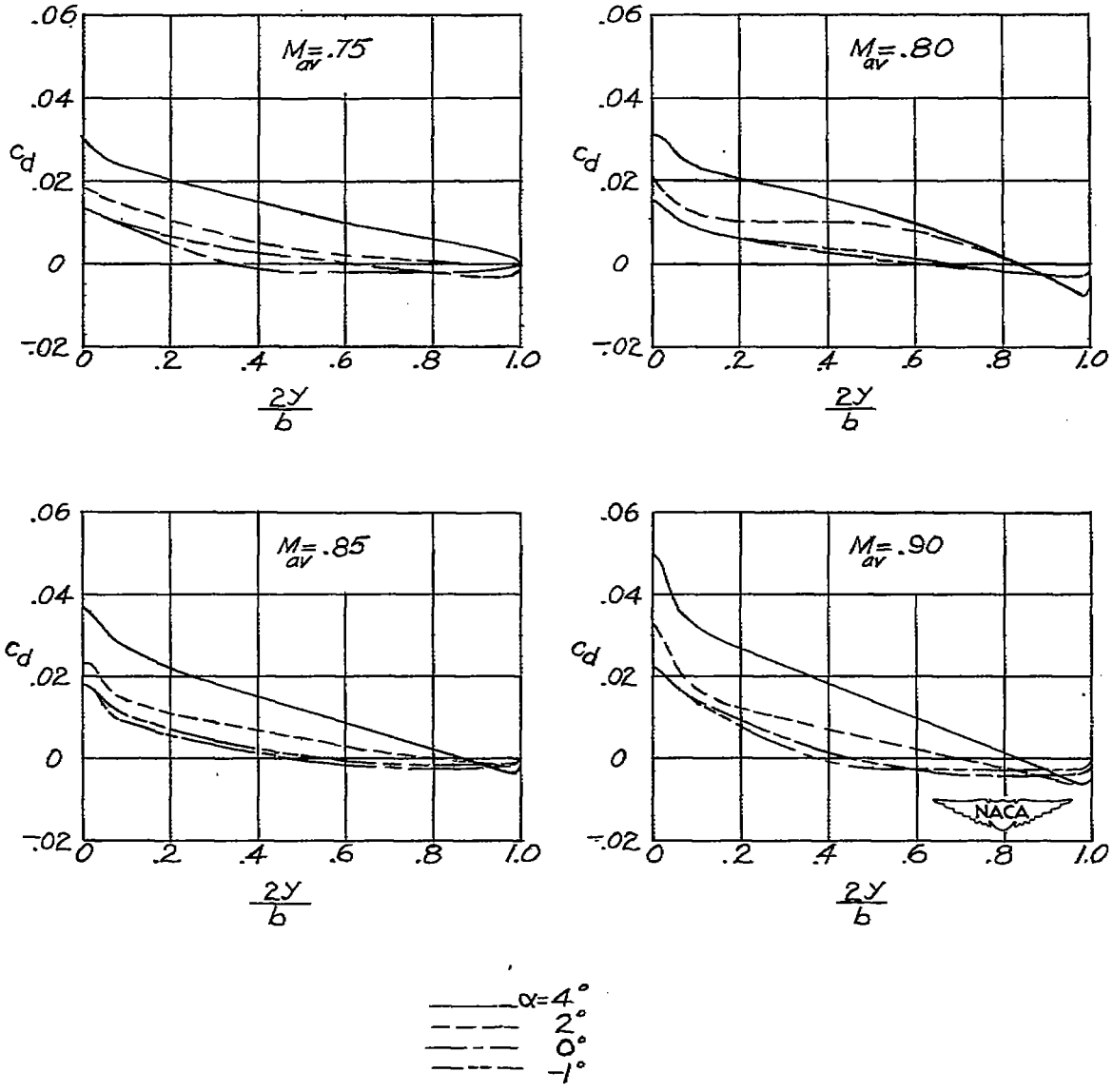

(a) M_{av} = 0.75 to 0.90.

Figure 13.- Spanwise variation of section pressure-drag coefficient for selected average Mach numbers and angles of attack.

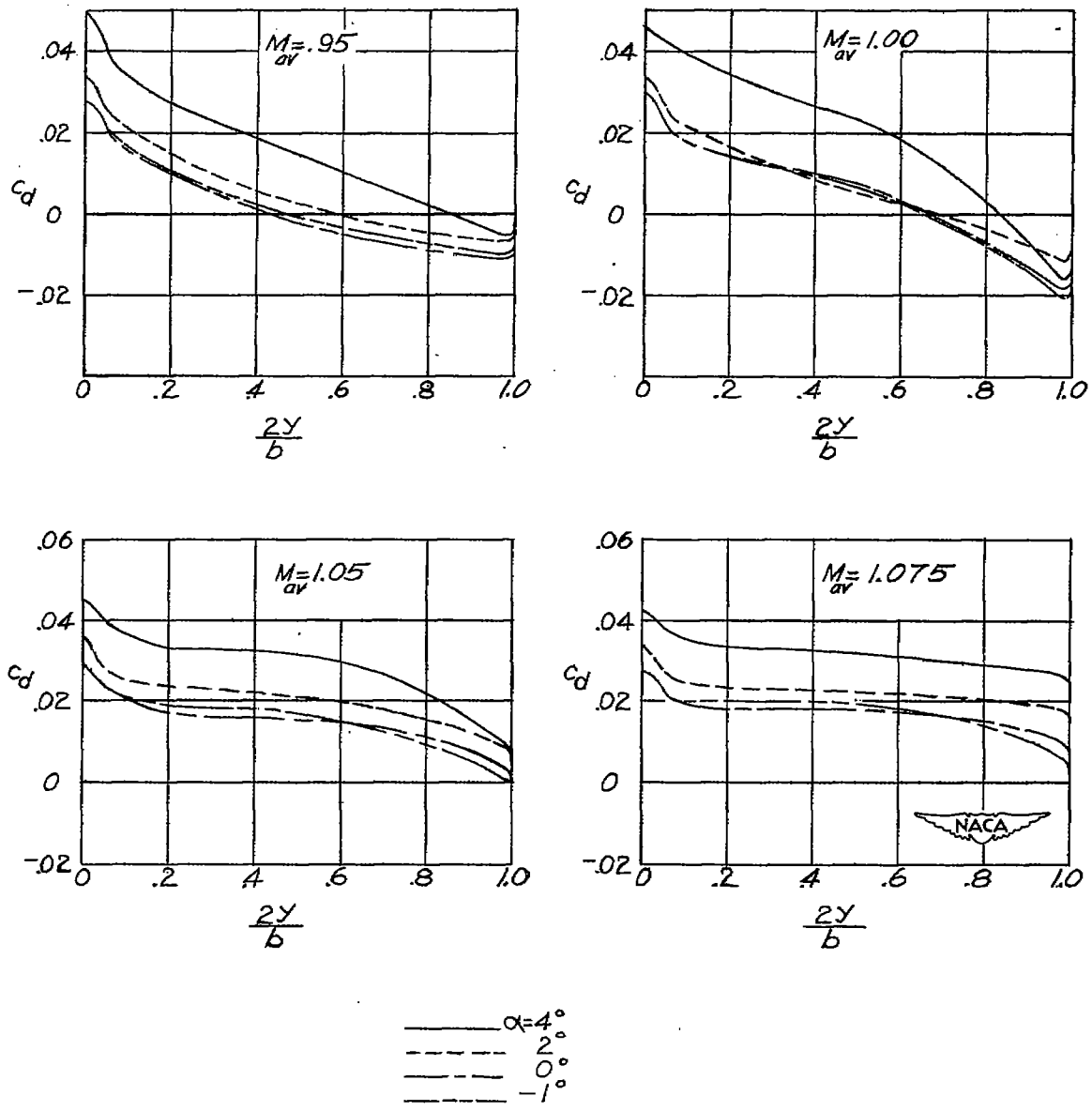

(b) M_{av} = 0.95 to 1.075.

Figure 13.- Concluded.

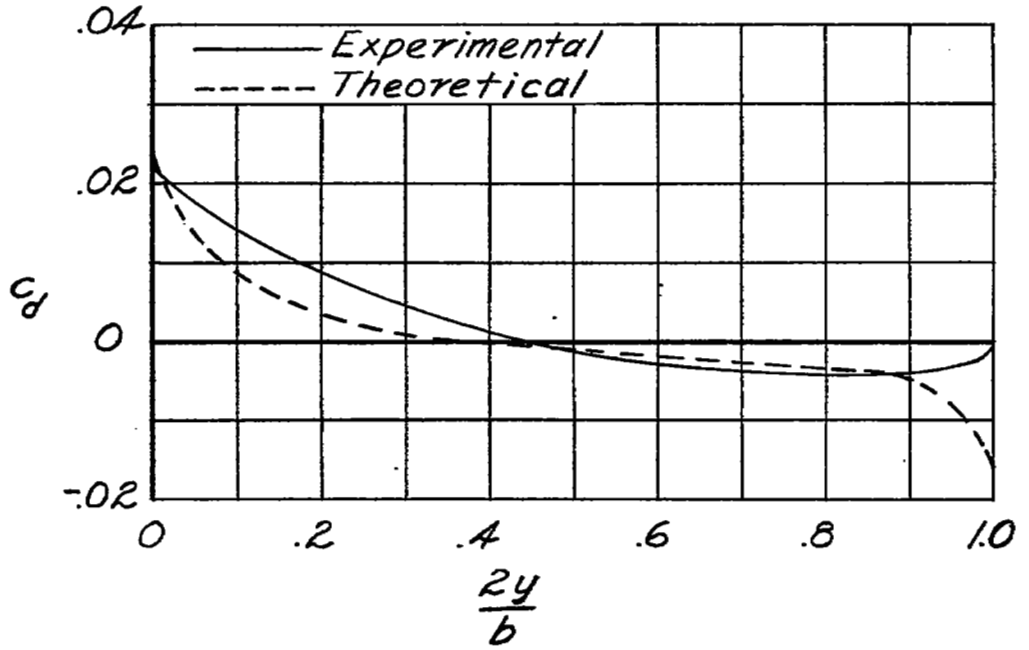

(a) M_{av} 0.90.

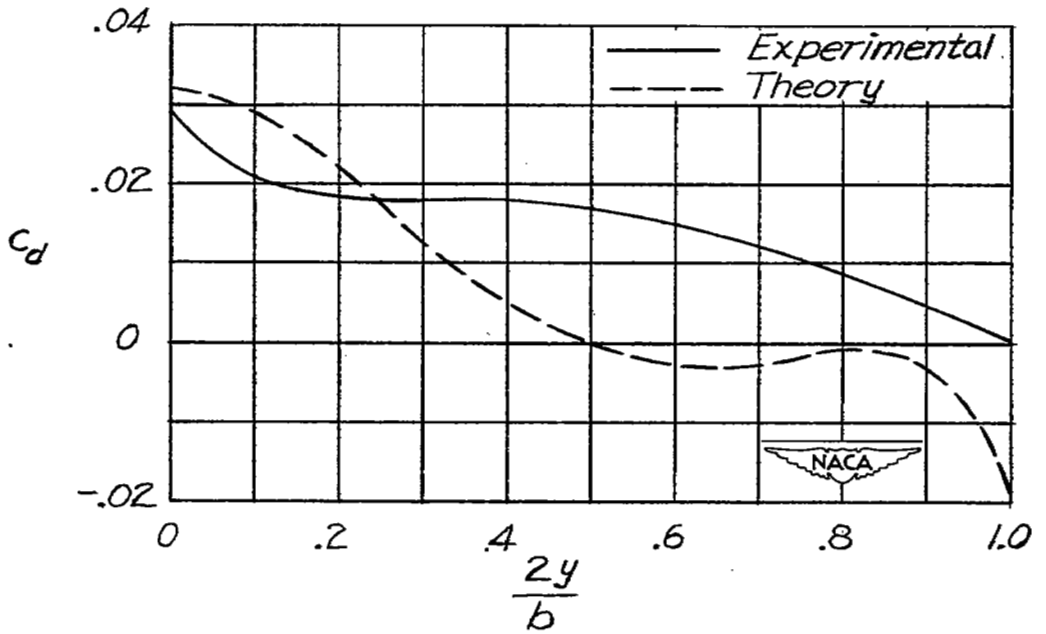

(b) M_{av} 1.05.

Figure 14.- Comparison of experimental and theoretical spanwise drag distributions at zero lift.

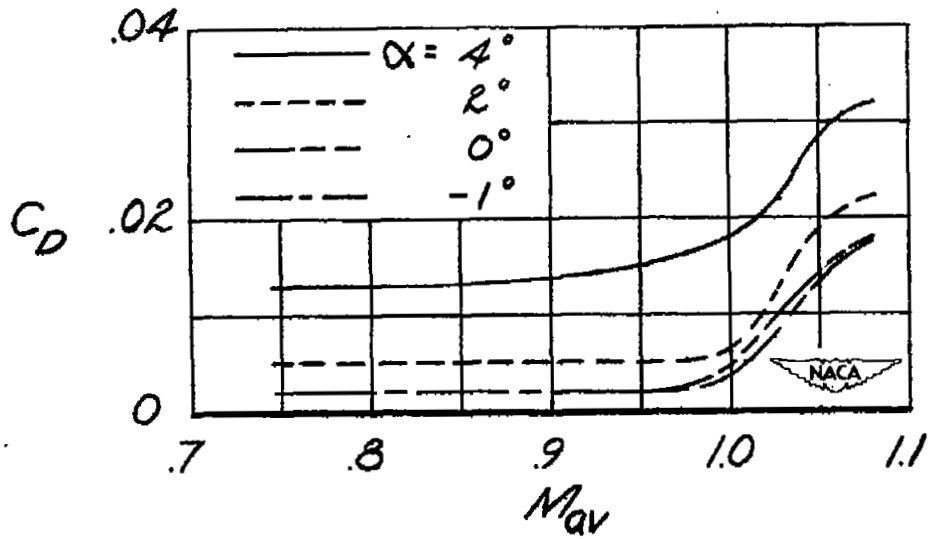

Figure 15.- Variation of wing pressure-drag coefficient with Mach number for several angles of attack.

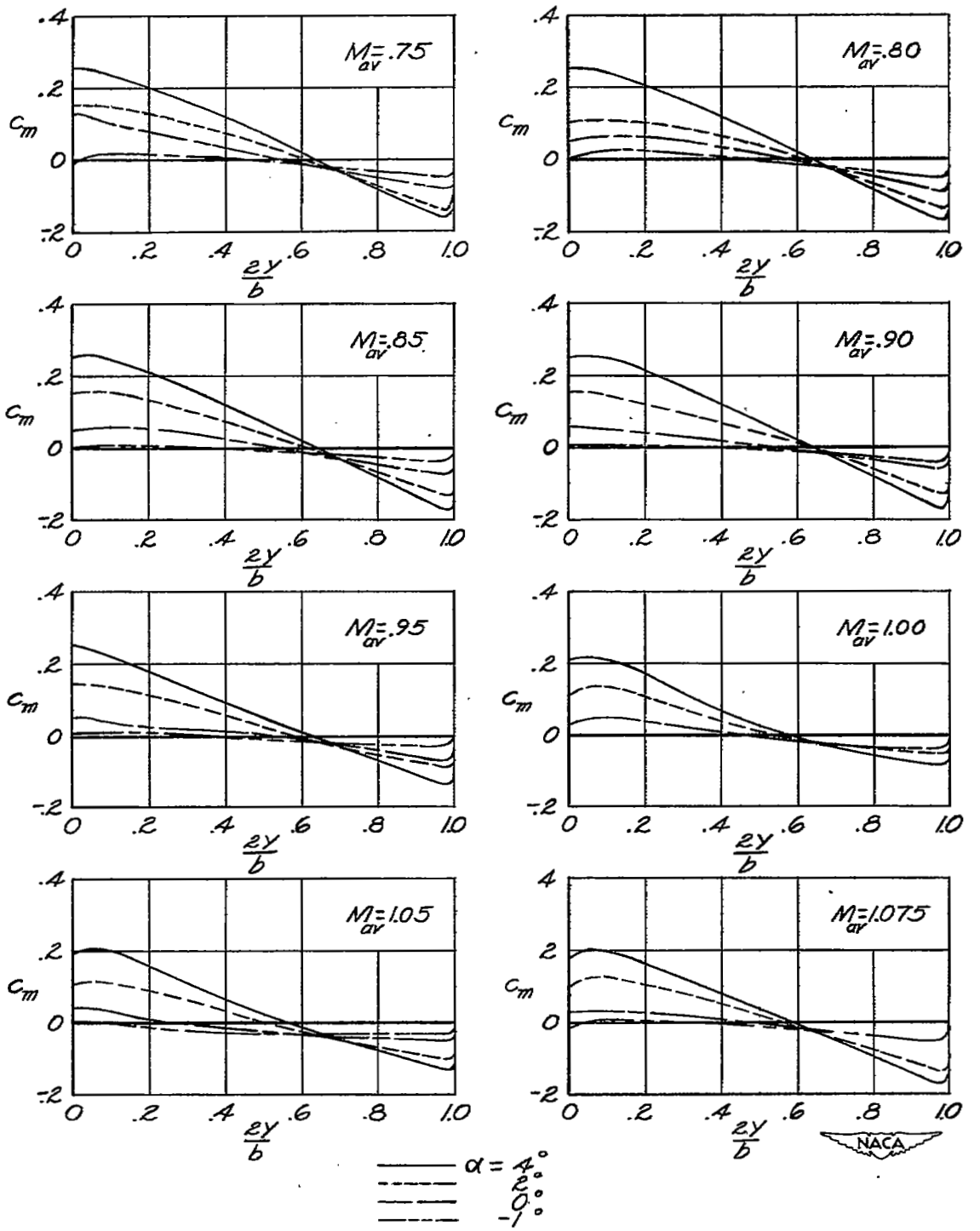

Figure 16.- Spanwise variation of section pitching-moment coefficient for selected Mach numbers and angles of attack.

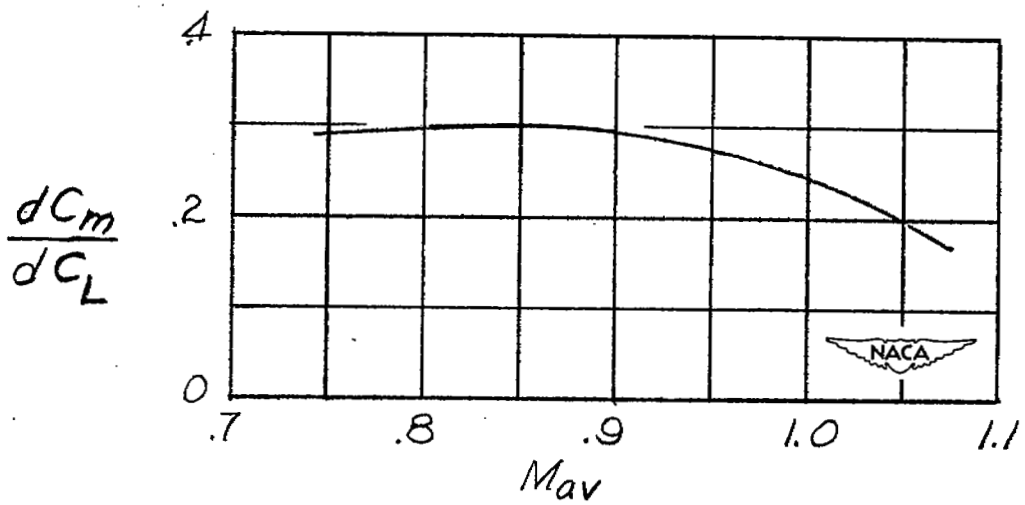

Figure 17.- Variation of $\frac{dC_m}{dC_L}$ with average Mach number.

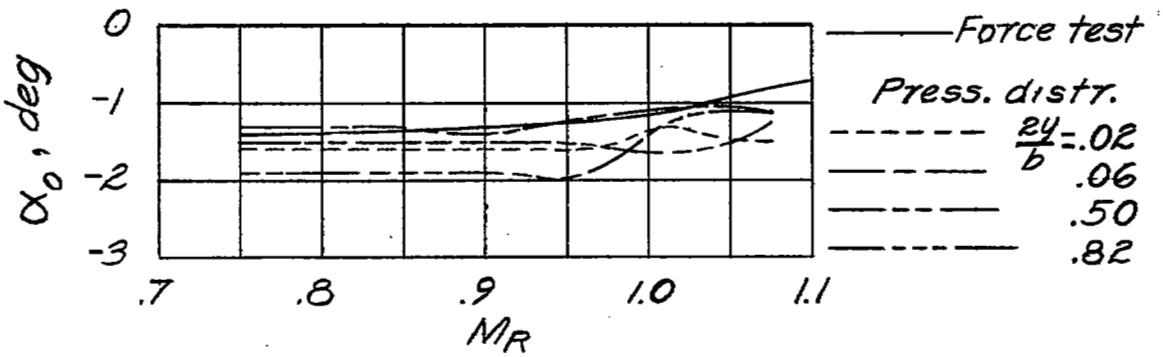

(a) α_o as a function of M_R.

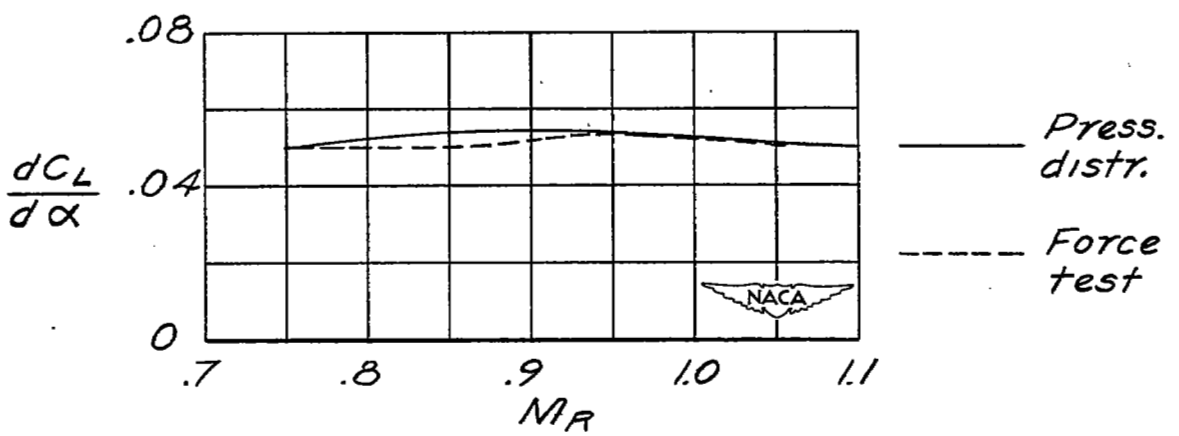

(b) $\frac{dC_L}{d\alpha}$ as a function of M_R.

Figure 18.- Comparison of results of pressure-distribution measurements with force-test results.

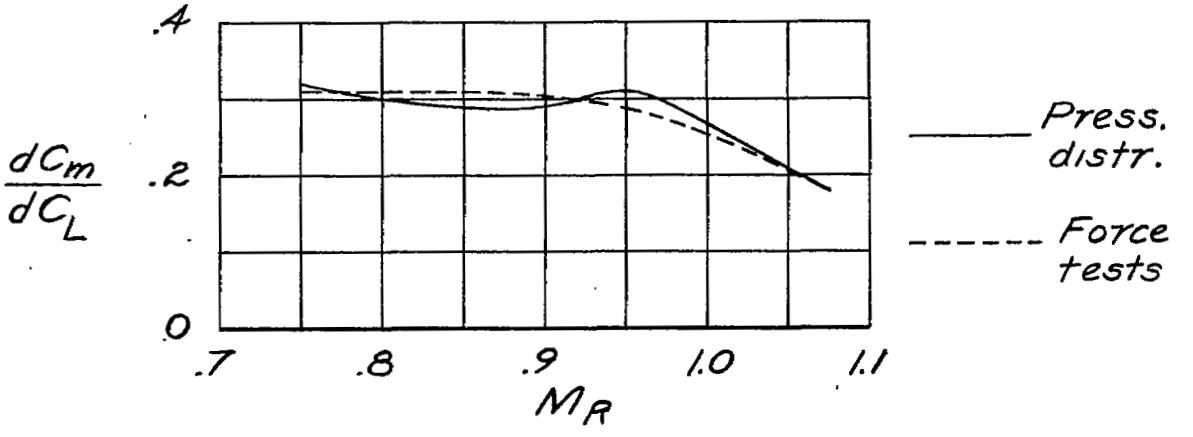

(c) $\frac{dC_m}{dC_L}$ as a function of M_R.

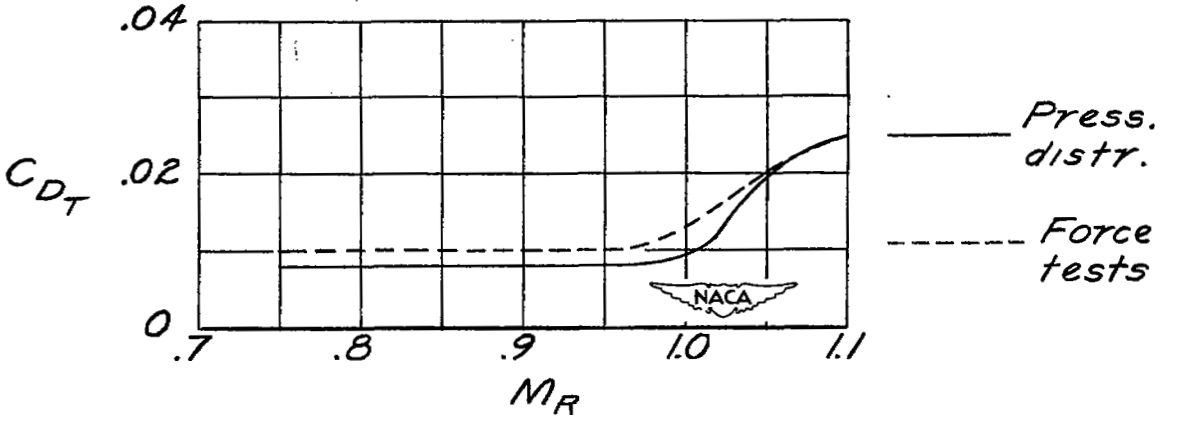

(d) Total drag coefficient C_{D_T} as a function of M_R.

Figure 18.- Concluded.

NACA-Langley - 6-25-51 - 390

NASA Technical Library
3 1176 01436 8618

[redacted]